9950-874

ARKANSAS
REMOTE SENSING
LABORATORY

EVALUATION OF SIR-A SPACE RADAR FOR GEOLOGIC INTERPRETATION: UNITED STATES, PANAMA, COLOMBIA, AND NEW GUINEA

FINAL REPORT

By

H. MacDonald
W.P. Waite
V.H. Kaupp
L.C. Bridges
M. Storm

(NASA-CR-173121) EVALUATION OF SIR-A SPACE RADAR FOR GEOLOGIC INTERPRETATION: UNITED STATES, PANAMA, COLOMBIA, AND NEW GUINEA Final Report (Arkansas Univ.) 84 p HC A05/MF A01 CSCL 08B G3/43

N83-35469

Unclas
42161

August, 1983

JPL Contract No. 954940

ARSL TR 83-2

This work was performed for the Jet Propulsion Laboratory, California Institute of Technology, sponsored by the National Aeronautics and Space Administration under Contract NAS7-918 (Task Order No. RD-185)

UNIVERSITY OF ARKANSAS

FAYETTEVILLE, ARKANSAS 72701

EVALUATION OF SIR-A SPACE RADAR FOR GEOLOGIC INTERPRETATION: UNITED STATES, PANAMA, COLOMBIA, AND NEW GUINEA

FINAL REPORT

By

H. MacDonald
W.P. Waite
V.H. Kaupp
L.C. Bridges
M. Storm

August, 1983

JPL Contract No. 954940

ARSL TR 83-2

This work was performed for the Jet Propulsion Laboratory, California Institute of Technology, sponsored by the National Aeronautics and Space Administration under Contract NAS7-918 (Task Order No. RD-185)

CONTENTS

LIST OF ILLUSTRATIONS

SECTION 1

SECTION 2

SECTION 3

SECTION 4

This report contains information prepared by the University of Arkansas under JPL sub-contract. Its content is not necessarily endorsed by the Jet Propulsion Laboratory, California Institute of Technology, or the National Aeronautics and Space Administration.

ABSTRACT

Future spaceborne imaging radars are expected to join Landsat-type systems for global remote sensing and geologic reconnaissance mapping. Seasat and SIR-A space (Shuttle) radars have clearly demonstrated the value of microwave remote sensing of both ocean and terrain surfaces. Traditionally, the dominant merits of radar remote sensing have long been an active mode of operation, and the independence from weather and solar illumination. One of the primary recognized advantages of radar for geologic reconnaissance mapping is radar's sensitivity to topography. However, the quality of radar imagery, particularly for geologic applications, is critically dependent on the slope and relief of the terrain as well as the look-angle (measured from nadir) of the imaging system.

Comparisons between Landsat MSS imagery, and aircraft and space radar imagery from different geologic environments in the United States, Panama, Colombia, and New Guinea demonstrate the interdependence of radar system geometry and terrain configuration for optimum retrieval of geologic information. Examples illustrated throughout this report would suggest that in the case of space radars (SIR-A in particular), the ability to acquire multiple look-angle/look-direction radar images of a given area is more valuable for landform mapping than further improvements in spatial resolution. Radar look-angle is concluded to be one of the most important system parameters of a space radar designed to be used for geologic reconniassance mapping. It is important, therefore, to determine the optimum set of system parameters for imaging different classes of landform features, and tailoring the look-angle to local topography.

SIR-B will be the first orbital imaging radar system capable of providing multiple images of the same target at different look-angles. This unique capability used in conjunction with other image types provides a rare opportunity to determine optimum radar look-angles for world-wide geologic applications.

New Technology None

SECTION 1 SIR-A COMPARISONS, UNITED STATES

INTRODUCTION

The evolution of radar geology has been most significant during the last three decades. In the 1950's the use of imaging radars was mostly the privilege of the military, but the 1960's were highlighted by the development and declassification of side-looking radar (SLAR) systems. The introduction of the geologic community to high quality radar images in the mid-1960's led to the definition of capabilities and limitations and the establishment of a framework for radar geology. The 1970's were noteworthy because of the availability of commercial SLAR imagers, renewed involvement of NASA in microwave Earth resources applications, and of course the 1978 launch of NASA's first Earth orbiting radar system aboard the Seasat Satellite. Most recently (November 12, 1981) NASA launched Space Shuttle Columbia on its second orbital mission carrying the Shuttle Imaging Radar system (SIR-A).

Seasat and SIR-A imaging radars have clearly demonstrated the value of microwave remote sensing of both ocean and terrain surfaces (Elachi, 1980; Ford, 1980; Ford et al., 1980). SIR-A imagery in particular has provided an important and unique data contribution for geologic reconnaissance mapping in those geographic areas which have perpetual cloud cover and are relatively inaccessible (MacDonald, 1982; Elachi, 1982). Even where Landsat imagery is available, spaceborne radars have provided complementary geologic information (Ford, Cimino, and Elachi, 1983; Elachi et al., 1982; McCauley et al., 1982; and Waite et al., 1981). Spaceborne

imaging radars will become as commonly used in geologic investigation as have Landsat images. However, timely development of this application necessitates a scientific basis for exploiting the sensitivity of radar reradiation to various aspects of the geologic terrain. In this study, comparisons between aircraft and space radars are provided to demonstrate the interdependence of radar design and terrain configuration for optimum retrieval of geologic information.

BACKGROUND

The dominant merits of radar remote sensing have long been held to be the active mode of operation, the independence from weather and solar illumination, and the enhancement of topographic relief (landforms) through shadowing. Early research in radar geology applications used airborne systems, and in order to obtain any appreciable swath of coverage from aircraft altitudes, moderate to large look-angles (measured from nadir, Fig. 1) were a necessity. Consequently, the bulk of all radar imagery examined by geoscientists was obtained at relatively large look-angles. This is likewise precisely the mode of operation that produces shadow enhancement of landforms which is particularly advantageous for geologic applications. It is also the look-angle range where geometric fidelity greatly improves. In contrast, radar imagery obtained at relatively small look-angles exhibits pronounced foreshortening and layover in high relief areas. These considerations led to an historical consensus that the best look-angle for geologic applications was that which provided sufficient shadow to enhance the topography, but not enough to

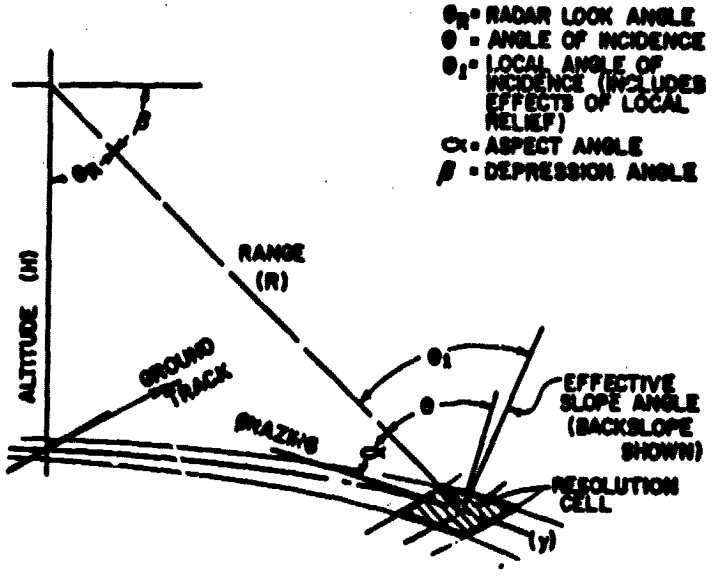

Figure 1. Imaging radar geometry (After Kaupp, Waite, and MacDonald 1982).

cause excessive data loss. In planning satellite radar missions for geologic applications this same reasoning has been applied, even though the maximum look-angle is restricted to approximately 60° because of hardware limitations. The usual recommendation has been to operate with the largest practical look-angle to obtain maximum enhancement.

Several new developments have since occurred that have caused re-examination of this conclusion. First, a large amount of high quality Seasat imagery at a look-angle of approximately 20°±3° has become available to the scientific community. This imagery of land areas has been, if anything, far better than expected, particularly in regions of relatively low slope and relief. The enhancement of subtle landform features is related to Seasat's operation in the range of relatively rapid variation of $\sigma°$, and the consequent sensitivity to moderate changes in slope. The radar backscatter $\sigma°$, is the percentage of return signal determined

by the electromagnetic properties of the terrain and local angle of incidence. Examination of Figure 1 illustrates the relationship between look-angle and local angle of incidence. When the terrain is flat and the imaging radar system not influenced significantly by the Earth's curvature, the incidence angle and look-angle are equal (Fig. 1). However, the local angle of incidence, the angle defined between the incident beam and a perpendicular to the true terrain slope, includes the effect of local relief. As can be seen in Figure 2, in the 30° and 70° local angle of incidence range, the typical backscatter curve is relatively flat. Small changes in terrain slope in the incidence angle ranges of less than 30° or more than

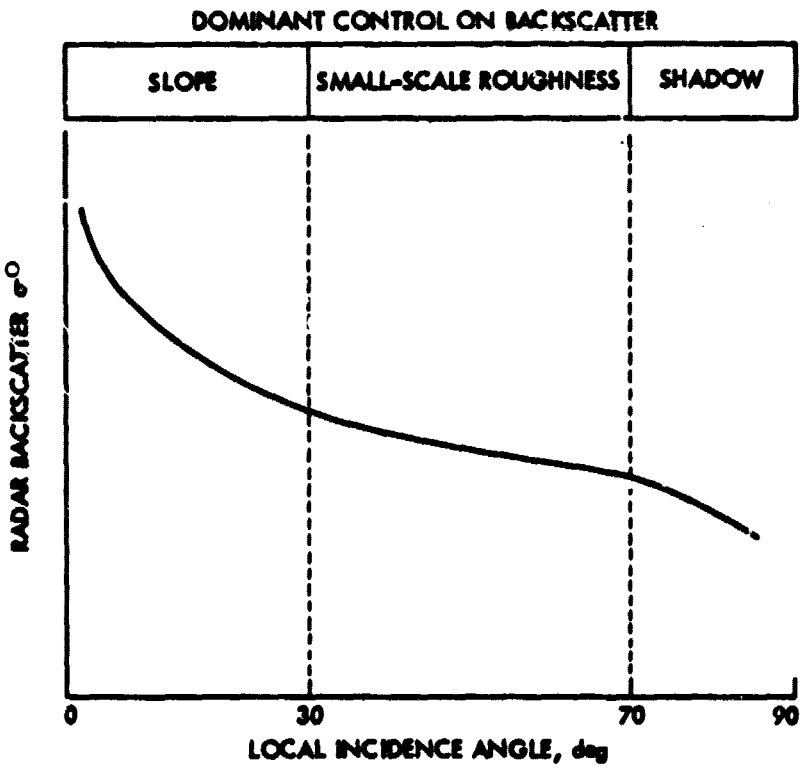

Figure 2. Generalized radar backscatter curve (After Ford, Cimino, and Elachi, 1983).

70° result in relatively large variations in radar backscatter and consequently, tonal contrasts on the imagery. For a given scale of roughness, relatively smaller incidence angles provide for higher backscatter.

In addition to the availability of small look-angle Seasat imagery, the lack of controlled data over a wide range of system and surface configurations has been supplemented by a developing program of radar image simulation (Kaupp, Waite, and MacDonald, 1982). The significance of radar look-angle becomes apparent when comparing radar imagery of similar terrain obtained with spacecraft and aircraft systems. The quality of radar imagery, particularly for many geologic applications, will be shown to be particularly dependent on tailoring the look-angle to terrain slope and relief.

LOOK - ANGLE COMPARISONS

Bunker, Missouri Area

Bunker is in the Ozark Uplift Province of Missouri approximately 140 km southwest of St. Louis. The area of essentially flat-lying carbonate strata has been highly dissected into basic dendritic stream patterns. Maximum relief is approximately 150 m with slopes averaging 10°, and the uniform vegetative cover is a mix of deciduous forest. Figure 3A is a Ka-band (0.86 cm wavelength) aircraft radar image which provides a striking contrast with the L-band (23 cm wavelength) spaceborne SIR-A image (Fig. 4A) of the same area. The look-angles for the aircraft image were approximately 12°-73° near to far range respectively, whereas the look-angle for the SIR-A was centered on 47°±3°. Drainage and topographic

lineament maps (Figs. 3B, C and 4B,C) derived from these two images reveal

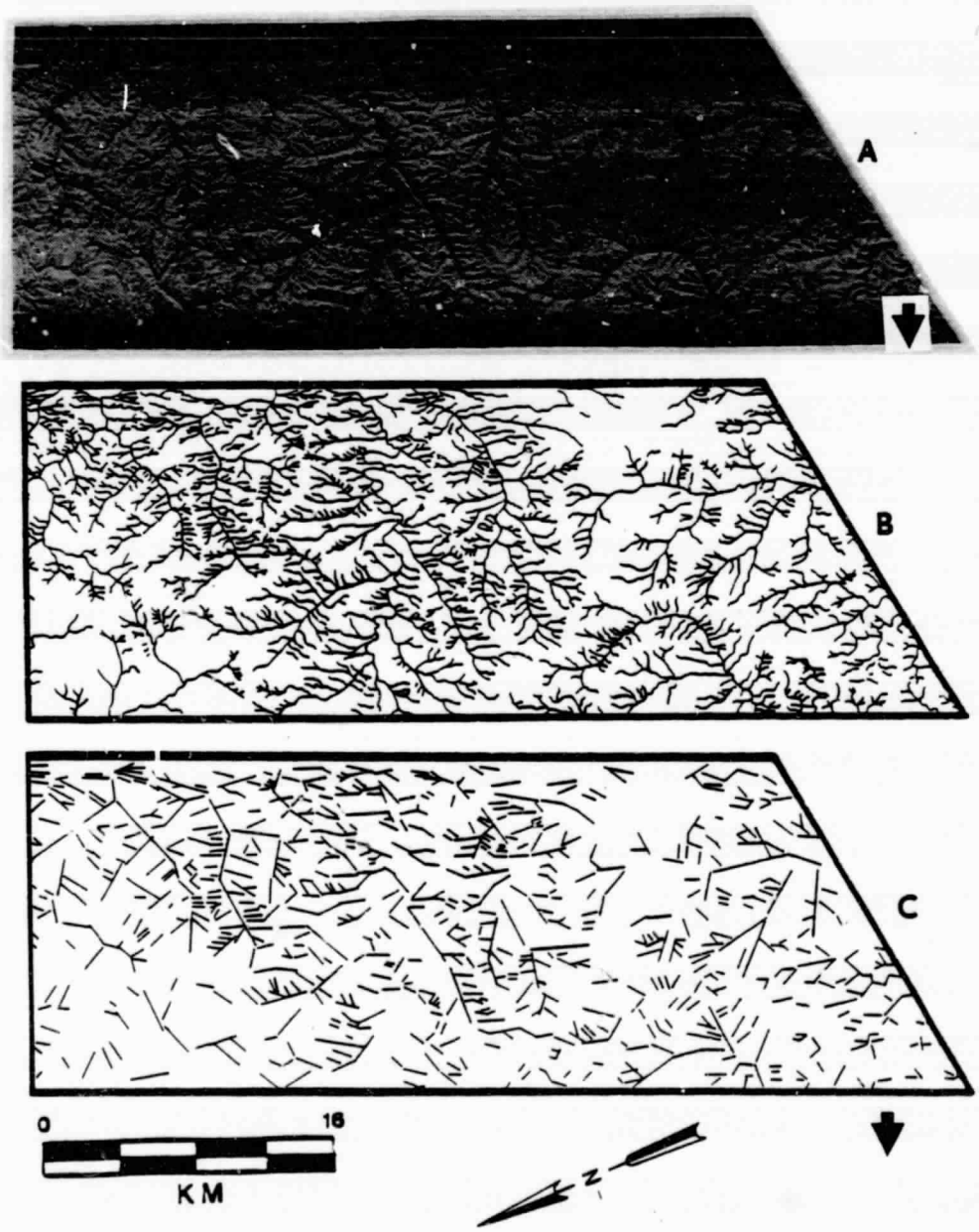

Figure 3. (A) aircraft imagery, (B) drainage patterns mapped from imagery, and (C) lineaments mapped from imagery.

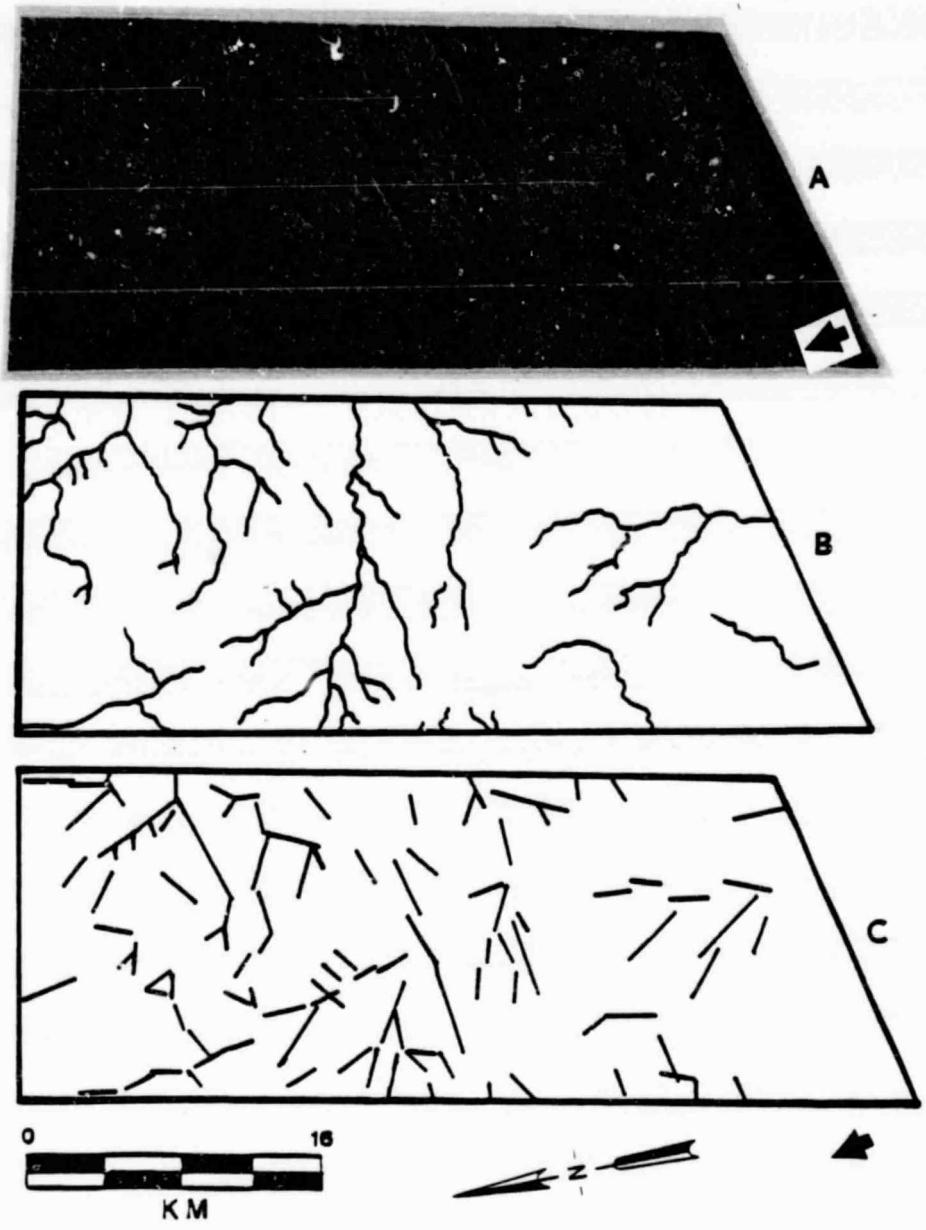

Figure 4. (A) SIR-A orbit 18, data take 22, (B) drainage mapped, and (C) lineaments mapped.

that there are insufficient tonal contrasts on the SIR-A image for mapping of anything but the larger stream channels and lineaments. There will be, of course, differences in the map products because of variation in radar illumination directions (look-directions, which are indicated by large

black arrows on the bottom of Figs. 3A and 4A), and also if low-order stream channels are narrower than the SIR-A resolution (40 m). However, by comparing a Landsat MSS image (Fig. 5) having a resolution almost twice (79 m) that of SIR-A, it becomes obvious that resolution is a relatively insignificant factor contributing to the inability of the SIR-A system to

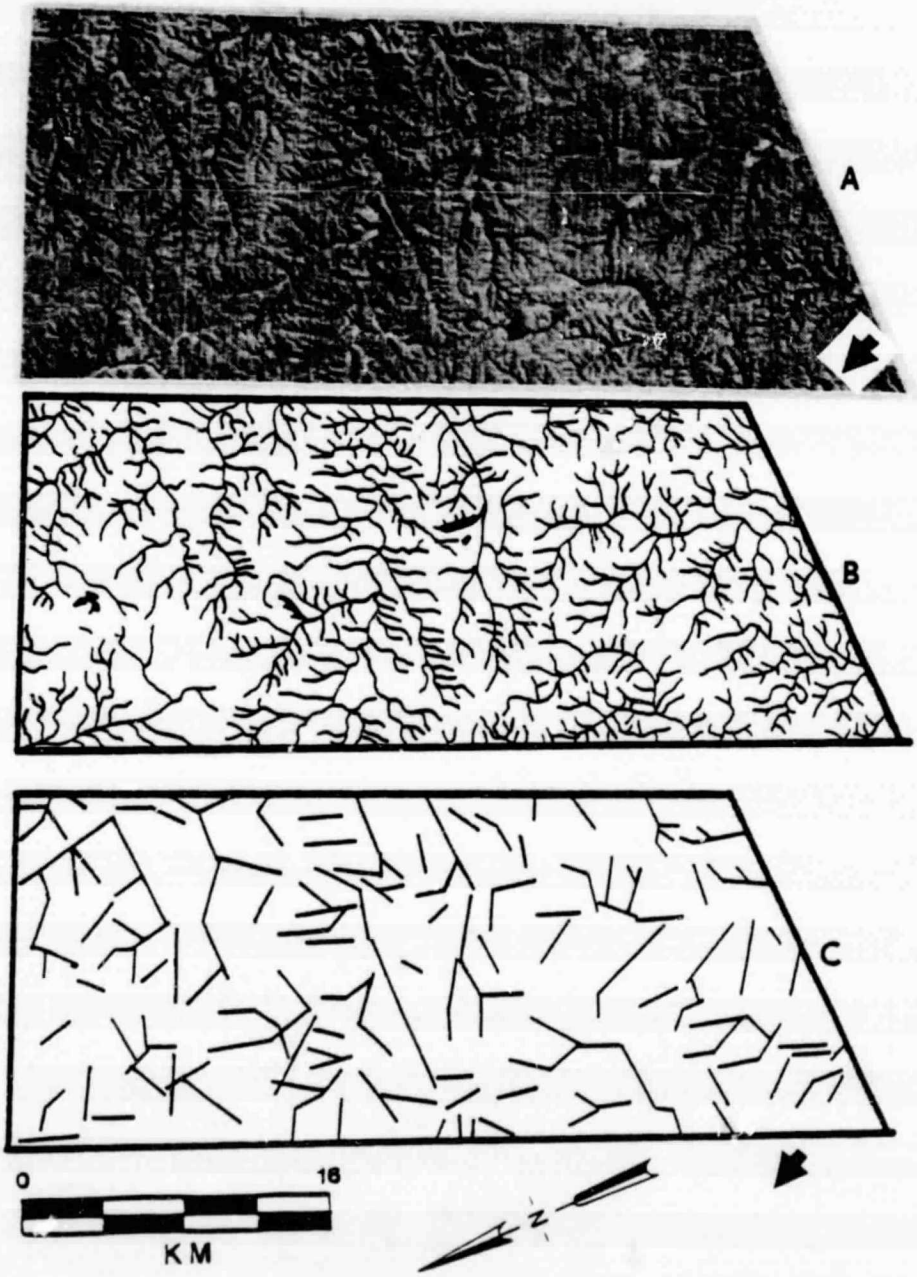

Figure 5. (A) Landsat MSS band 7, ID E-30235-16065; (B) drainage mapped; (C) lineaments mapped.

accentuate landform features in this terrain environment. The illumination directions for SIR-A and Landsat are somewhat similar (toward the north-northwest and northwest respectively) in contrast to that of the aircraft radar (toward the west); however, the significant factor is the illumination angle. The Landsat low sun elevation of 34° allows for solar highlighting of foreslopes and shading of backslopes. This landform enhancement by low solar elevation is somewhat analogous to the oblique illumination (large look-angles) utilized by many aircraft side-looking radar systems.

Ironton, Missouri Area

Located in the St. Francois Mountains of southeastern Missouri, the Ironton, Missouri area is characterized by exposures of igneous rocks (mostly granite and felsite) surrounded by dolomites and sandstones. The maximum relief is approximately 300 m with the steepest slopes averaging 15°. Similar to the Bunker, Missouri area the vegetative cover is mixed deciduous forest. However, unlike the aircraft/spacecraft comparisons previously discussed (Figs. 3 and 4), two space radar images are contrasted in Figures 6 and 7.

Although the SIR-A (Fig. 6) and Seasat (Fig. 7) space radars operated at the same frequency/wavelength (L-band, 23 cm), Seasat's increased sensitivity to subtle changes in slope is demonstrated by the improvement in detectability of drainage patterns and lineaments (Figs. 8 and 9). The contrasting discrimination of landforms on the Seasat versus SIR-A is related primarily to differences in look-angle and look-direction. The

impact of look-direction on lineament enhancement is illustrated by comparing the detectability of the north-trending lineament (R-S) on Figures 6 and 7. On Figure 7, the Seasat look-direction is nearly perpendicular

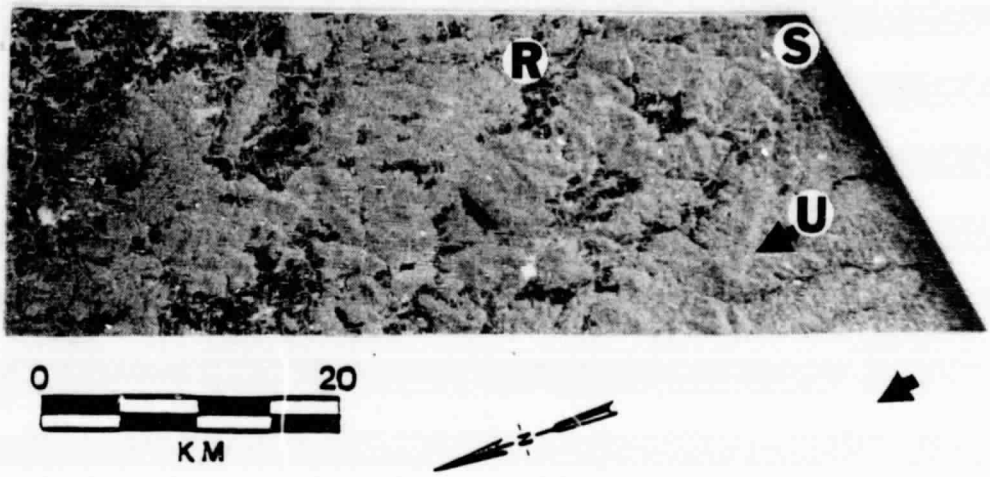

Figure 6. SIR-A image, orbit 18, data take 22.

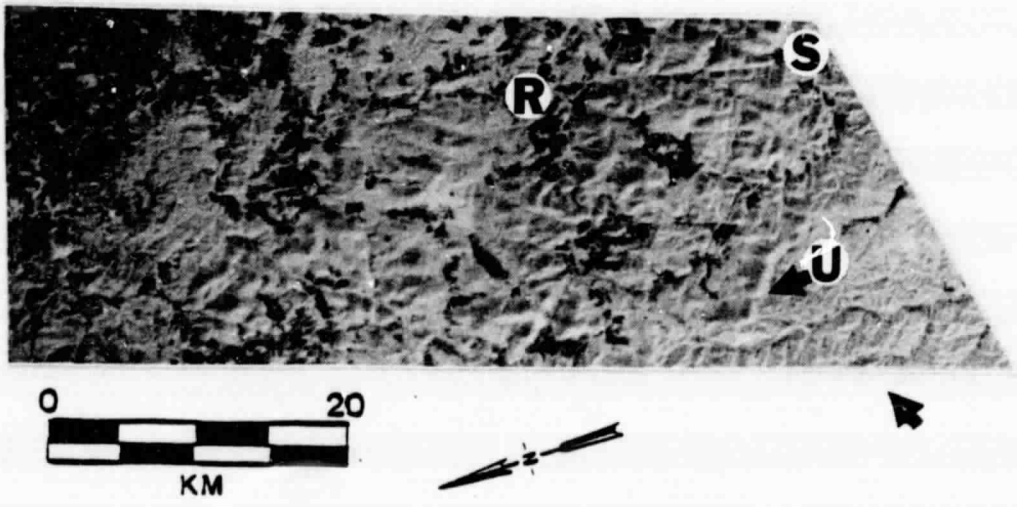

Figure 7. Seasat image, Rev. 723.

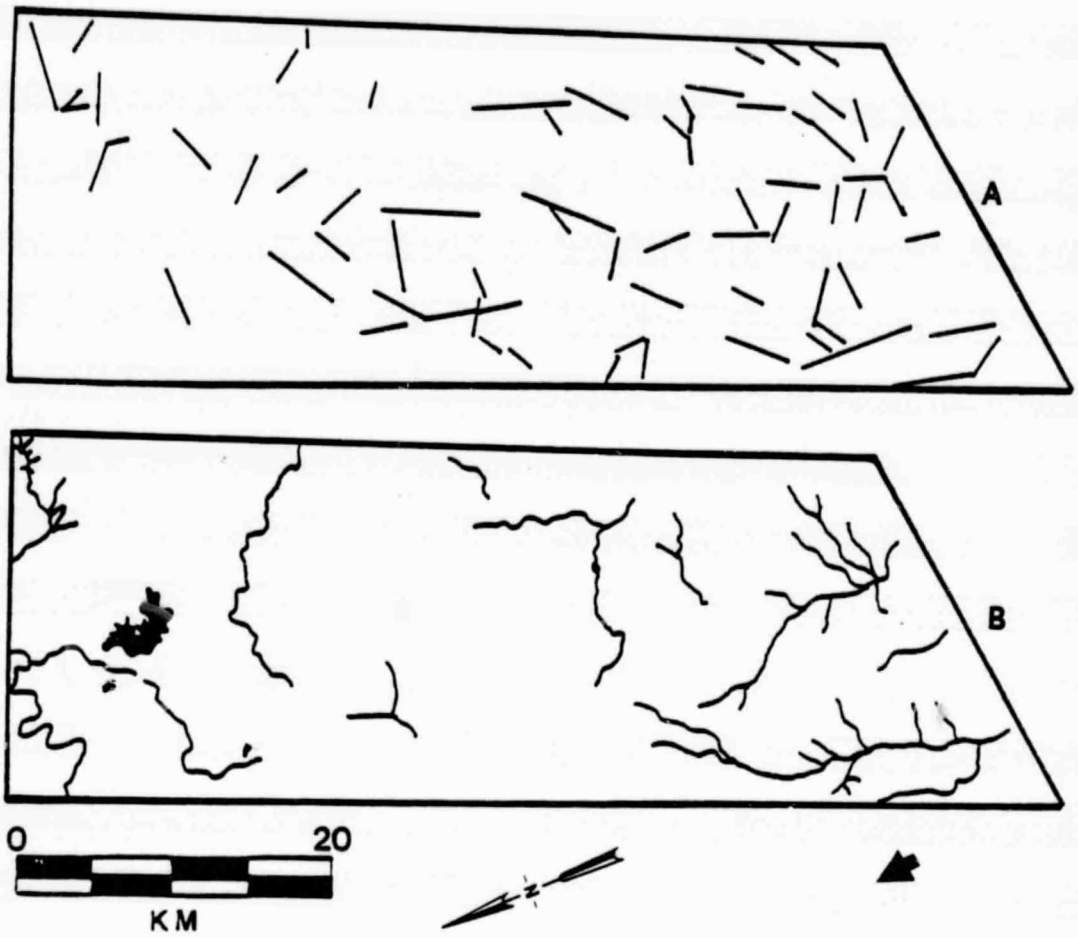

Figure 8. Mapped lineaments (A), and drainage patterns (B) from SIR-A image (Fig. 6).

to the lineament, whereas the continuity of the feature cannot be recognized on the SIR-A imagery (Fig. 6). The SIR-A look-direction is more nearly parallel to the feature. The highlighting of the lineament on the Seasat image is the result of a relatively small angle of incidence being formed by imaging terrain foreslopes at small look angles. The resulting enhanced contrast is also apparent in other areas on the Seasat imagery (for example, Area U Fig. 7) and this highlighting allows for an improve-

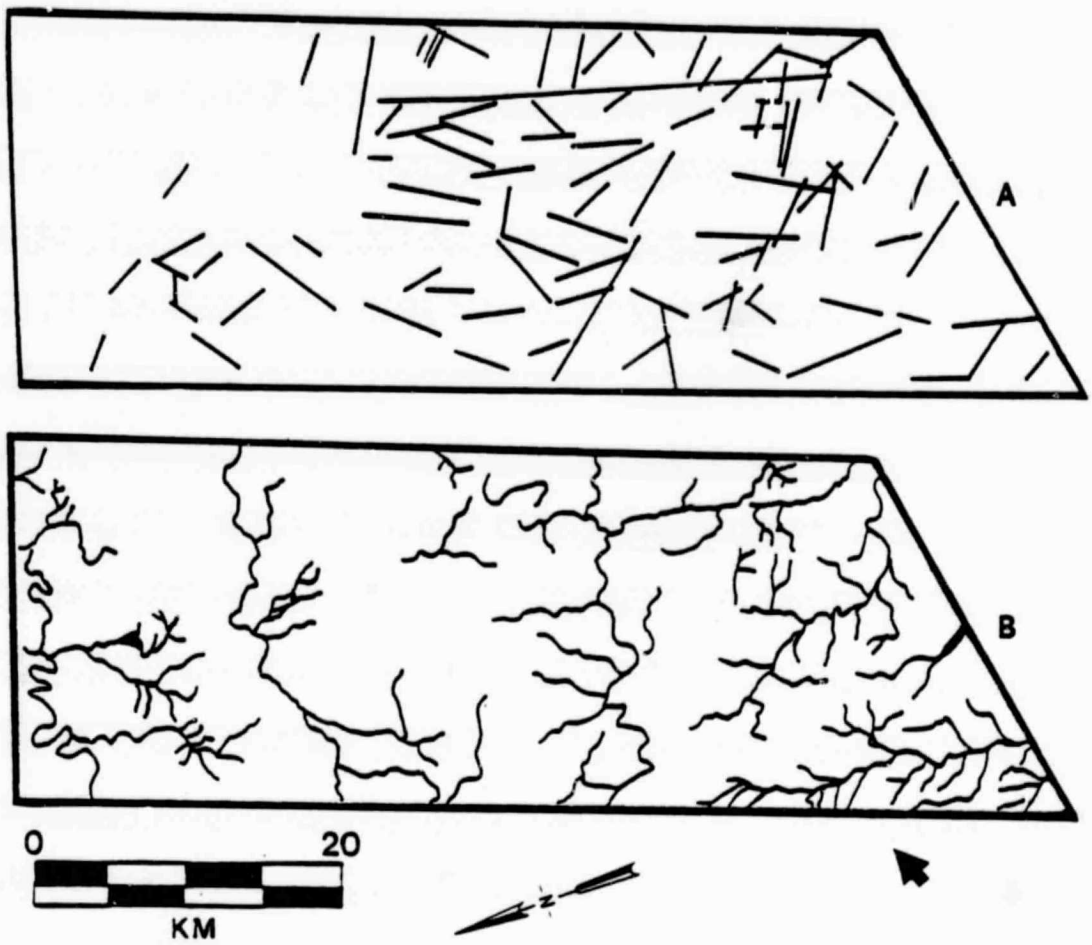

Figure 9. Mapped lineaments (A), and drainage patterns (B) from Seasat image (Fig. 7).

ment in drainage and lineament mapping over that of SIR-A. Because SIR-A's look-angles are centered on 47°±3°, subtle variations in terrain slope do not result in a range of local incidence angles that are sufficient to cause significant changes in backscatter. Consequently, in this terrain environment the SIR-A images provides relatively little landform discrimination.

Monongahela River Areas, Southwestern Pennsylvania

Although the resolutions of Seasat (25 m) and SIR-A (40 cm) are different, this system parameter is of little importance when comparing landform definition and enhancement. In support of this observation, compare Landsat MSS, Seasat and SIR-A images of gently rolling terrain (slopes averaging approximately 7° and relative relief of 30 m) along the Monongahela River south of Pittsburgh, Pennsylvania (Fig. 10). The low solar illumination provided by the Landsat image allows for the detection of a dendritic pattern (between area d-f, Figs. 10B and 11B) which is fairly perceptible on the Seasat image, but not recognizable on the SIR-A imagery. Landsat in this case, with the poorest resolution in comparison to SIR-A, provides for the best terrain definition and discrimination of drainage patterns (see for example, area g Figs. 11B and 11C). In this area the relative relief is 120 m and the slopes average 10°. Again, the relatively larger look-angle used by SIR-A places the local angle of incidence for most slopes on the flat part of the characteristic backscatter curve (Fig. 2).

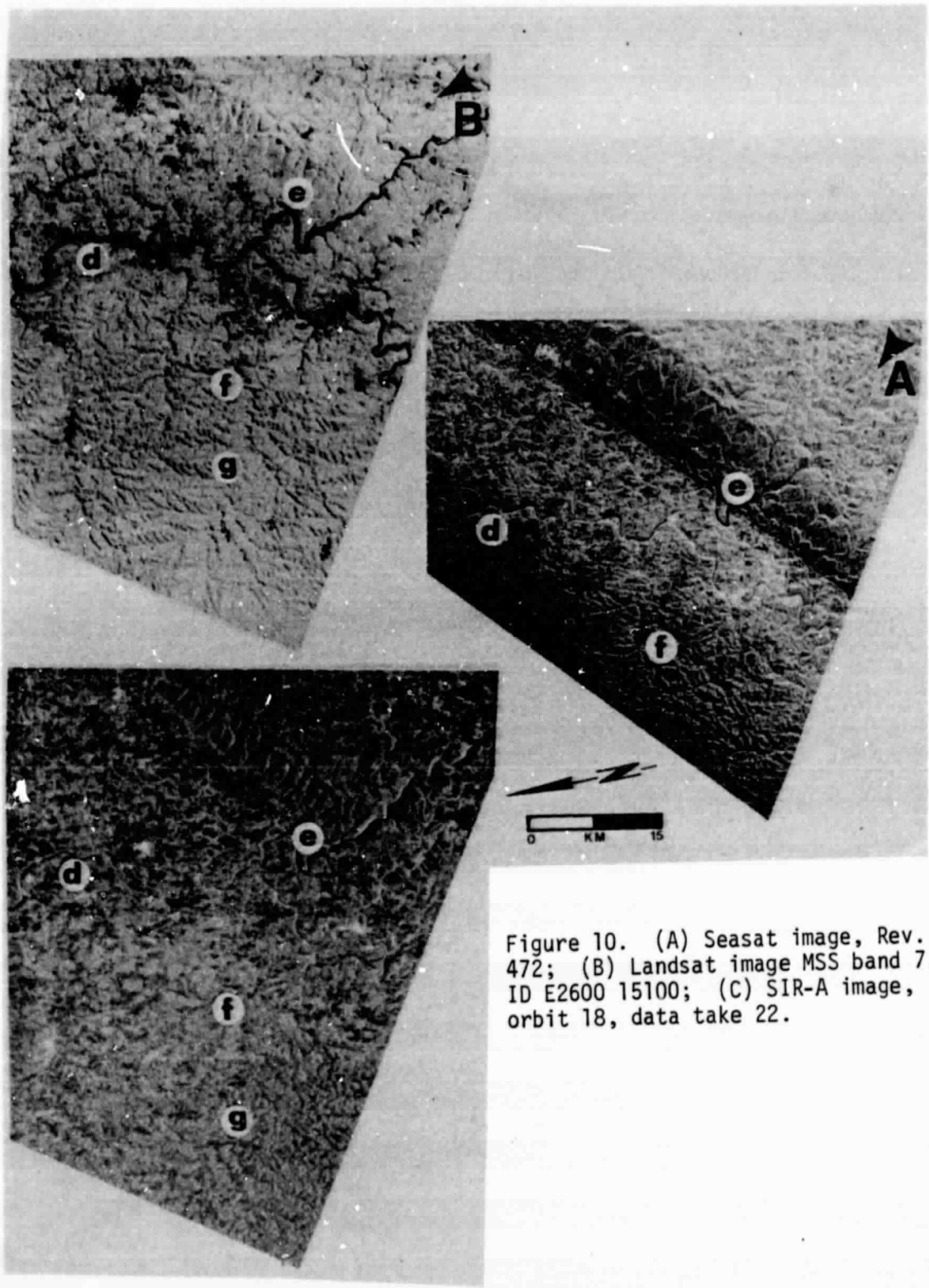

Figure 10. (A) Seasat image, Rev. 472; (B) Landsat image MSS band 7, ID E2600 15100; (C) SIR-A image, orbit 18, data take 22.

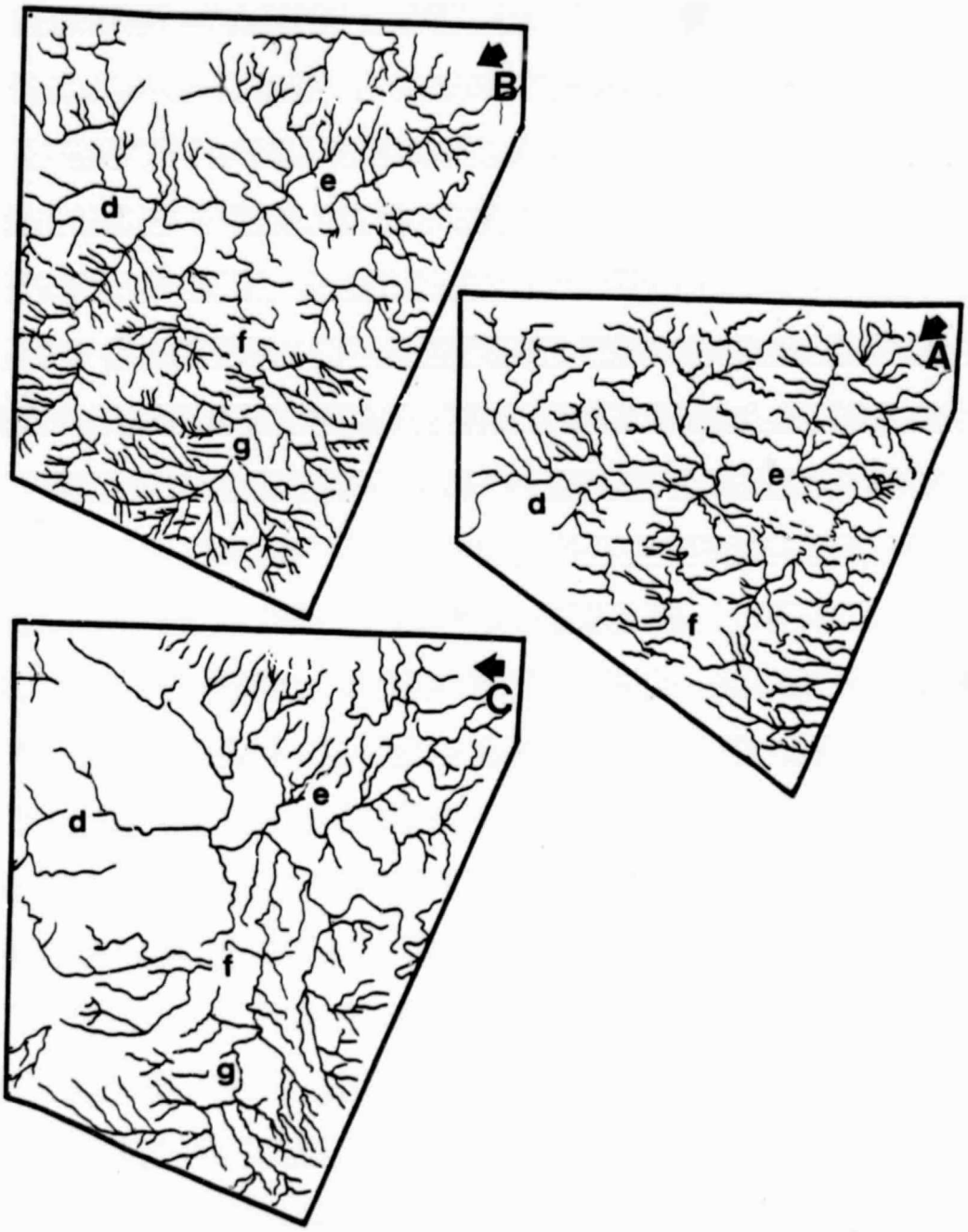

Figure 11. Drainage mapped from (A) Seasat, (B) Landsat, and (C) SIR-A.

St. Francois Mountains, Southeastern Missouri

Figures 12A and 12B provide a comparison between Landsat and SIR-A images that were obtained during similar seasons, but different years. The late October Landsat and early November SIR-A imagery again illustrate the significant impact look-angle plays in providing optimum landform definition.

The St. Francois Mountains (area A) are situated near the center of the Ozark Dome and consist of a core of exposed Precambrian granitic rocks. This region has been highly dissected and the topography reveals a significant amount of structural control as seen in the area between points A and B on the Landsat image (Fig. 12A). Numerous northeast trending lineaments are assumed to be normal faults associated with upwarping of the Ozark Dome. Relative relief is 100 m, with slopes averaging 12-14°. Accentuation of these lineaments has been reduced on the radar image because of SIR-A's look-angle. Even though the Landsat and SIR-A illumination angles (look-directions) are somewhat similar (toward the northwest), the highlighting and shadowing by a relatively low solar illumination angle (32°) is the key to landform definition and enhancement. Although the resolution of the Landsat image (79 m) is approximately twice that of SIR-A (40 m), mapping of drainage patterns from the Landsat image provides a significant improvement (Fig. 13A) over that of the SIR-A image (Fig. 13B). Accentuation of drainage patterns on the SIR-A imagery is reduced in comparison to the Landsat scene because radar return from subtle terrain differences fall on the flat part of the backscatter vrs. angle of incidence curve (Fig. 2).

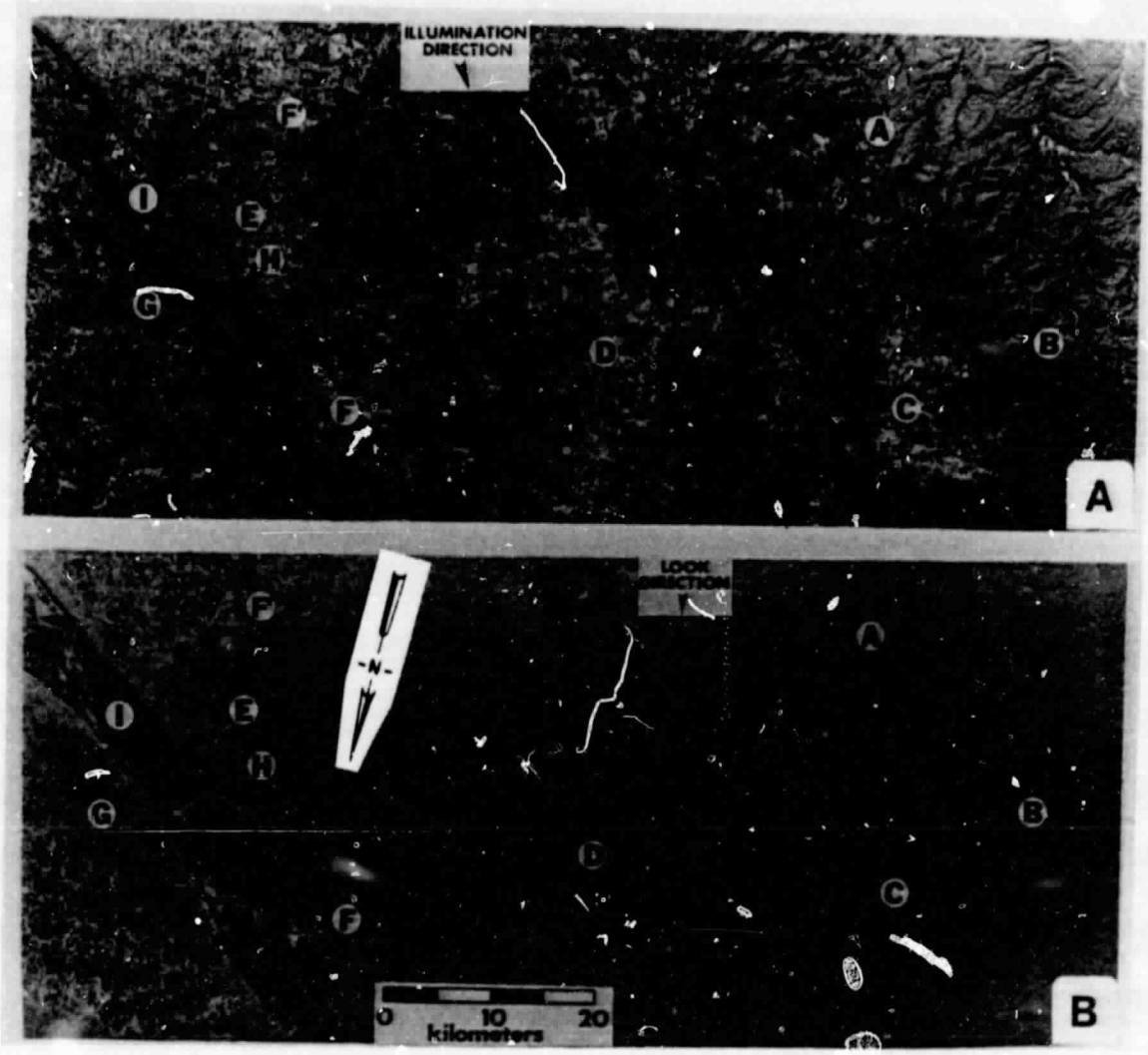

Figure 12. (A) Landsat MSS band 7, Oct. 21, 1977, solar elevation 32°, solar azimuth 140°, ID E-6003-15322; (B) SIR-A orbit 18, data take 22.

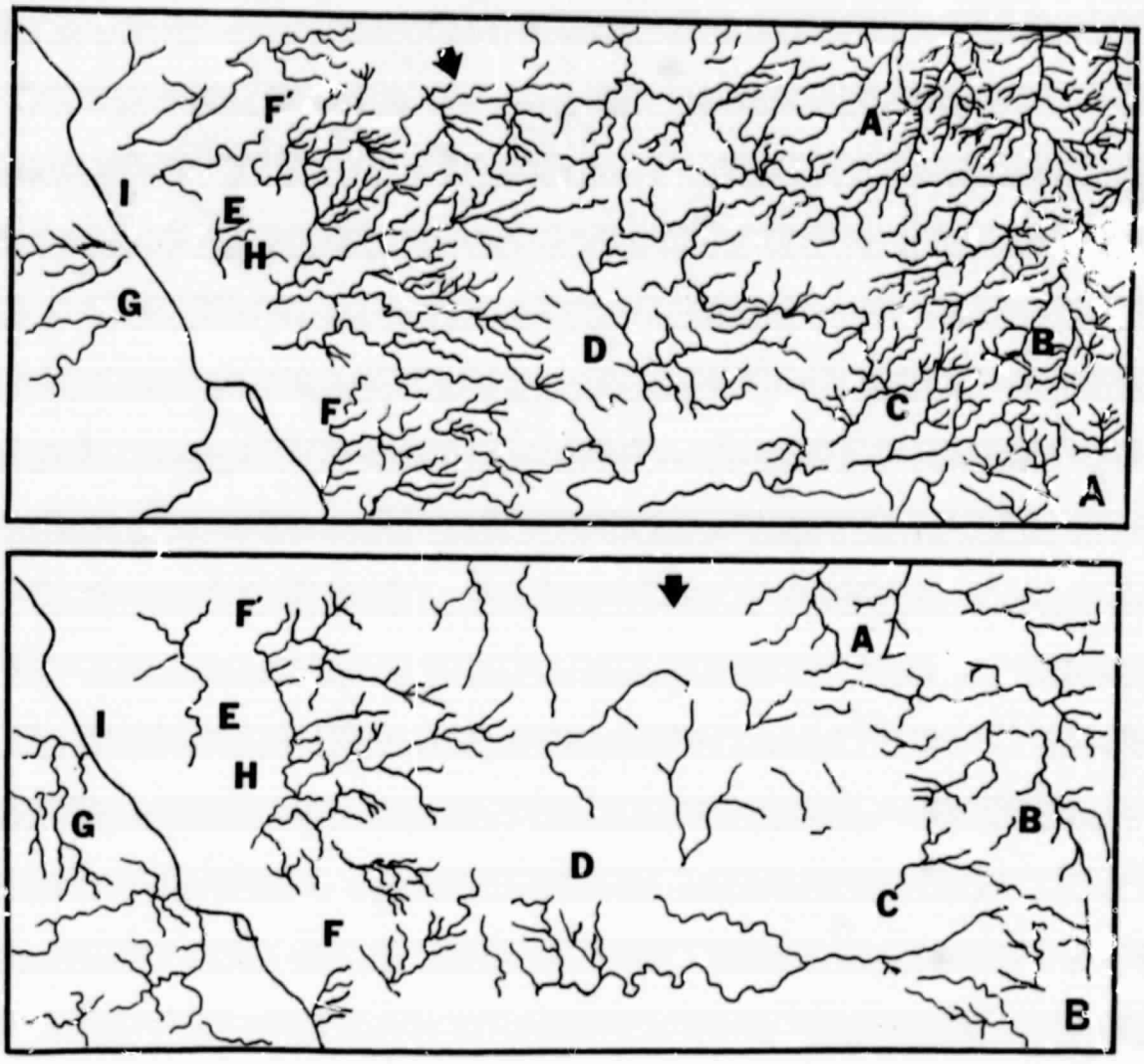

Figure 13. (A) Drainage mapped from Landsat, (B) drainage mapped from SIR-A.

REFERENCES SECTION 1

Elachi, C., 1980, Spaceborne Imaging Radar, Geologic and Oceanographic Applications: Science, Vol. 209, No. 4461, p. 1073-1082.

Elachi, C., 1982, Radar Images of the Earth from Space: Scientific American, Dec. 1982, p. 54-61.

Elachi, C., et al., 1982, Shuttle Imaging Radar Experiment: Science, Vol. 218, No. 4576, p. 993-1003.

Ford, J.P., 1980, Seasat Orbital Radar Imagery for Geologic Mapping: Tennessee-Kentucky-Virginia: AAPG Bull., Vol. 64, No. 12, p. 2064-2094.

Ford, J.P., et al., 1980, Seasat Views North America, the Caribbean, and Western Europe With Imaging Radar: JPL Publication 80-67, Jet Propulsion Laboratory, Pasadena, California, November, 1980.

Ford, J., J. Cimino, and C. Elachi, 1983, Space Shuttle Columbia Views the World With Imaging Radar: the SIR-A Experiment: JPL Publication 82-95, Jet Propulsion Laboratory, Pasadena, California, January, 1983.

Kaupp, V.H., W.P. Waite, and H.C. MacDonald, 1982, Incidence Angle Considerations for Spacecraft Imaging Radar: IEEE Trans. on Geoscience and Remote Sensing, Vol. GE-20, No. 3, p. 384-390.

MacDonald, H.C. (Contributing Author), 1982, Shuttle Imaging Radar-A (SIR-A) Experiment, in J.B. Cimino, and C. Elachi, Eds., NASA/JPL Publication 82-77, Dec. 1982, 85 p.

McCauley, J., et al., 1982, Subsurface Valleys and Geoarcheology of the Eastern Sahara Revealed by Shuttle Radar: Science, Vol. 218, No. 4576, p. 1004-1019.

Waite, W.P., H.C. MacDonald, V.H. Kaupp, and J.S. Demarcke, 1981, Wetland Mapping With Imaging Radars: International Geoscience and Remote Sensing Symposium (IGARSS'81) Digest, Vol. 2, p. 794-799, June, 1981.

SECTION 2 COMPLEMENTARY NATURE OF SPACE RADARS AND LANDSAT-TYPE IMAGERY FOR GEOLOGIC ANALYSIS

Virginia Dale Ring-Dike Complex, Colorado (N40°30' to 41°10' Lat., and W105° to 105°45' Long.)

The Virginia Dale ring dike complex, consisting of Precambrian granites and monzonites, is located in the center of the extreme south end of the Laramie Range at its juncture with the Colorado Front Range on the Colorado - Wyoming border (Fig. 1). The complex is geomorphically defined

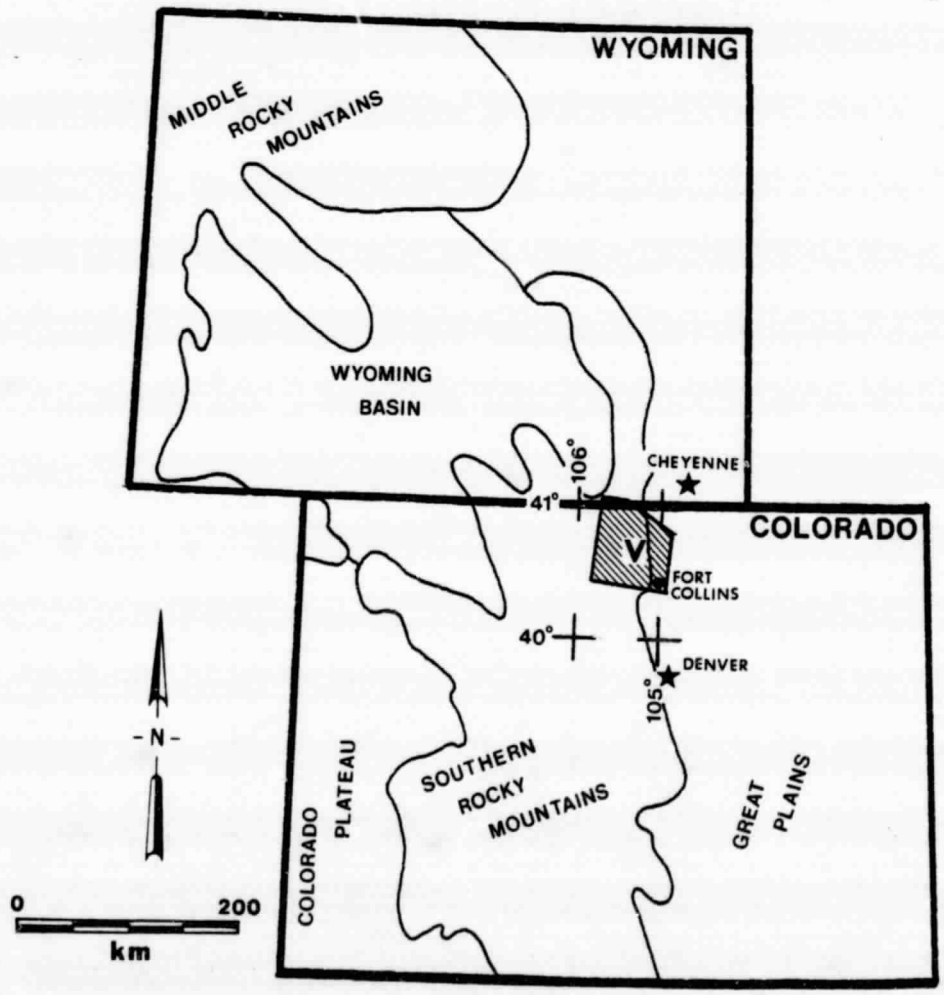

Figure 1. Location map, Virginia Dale ring dike complex area.

by a circular outcrop pattern (area D Fig. 2) approximately 14 km in diameter, and by a deeply eroded stream valley system reflecting a characteristic annular drainage pattern. The maximum relative relief within the entire study area is 1465 m. Figures 2, 3, and 4 allow for comparison between geologic information inferred from a Landsat image (Fig. 2) and two different space radar images (Fig. 3, Seasat; Fig. 4, SIR-A).

The importance of radar look-direction for detecting geologic features becomes immediately evident when contrasting inferred lineaments from the different images. For example, the lineament inferred between points C and D on the Landsat image (Fig. 2) and Seasat image (Fig. 3) is not apparent on the SIR-A image (Fig. 4). This lineament is approximately 30 km. in length and trends N13°E. The look-direction (solar azimuth) of the Landsat is toward N31°W, and the Seasat look-direction is toward N68°E, thus the illumination azimuths (angle between illumination direction and the landform trend) are 44° and 55°, respectively. As a result of these relatively large illumination azimuth angles, highlighting and shadowing are produced which enhance the lineament. The look-direction of SIR-A is toward N10°E which is essentially parallel to the trend of the feature. In this situation highlighting and shadowing are minimized and enhancement is greatly suppressed.

Another example of look-direction bias can be seen within the ring-dike complex. On the SIR-A and the Seasat images, there are several linear features (indicated by the arrows on Figs. 3 and 4) that trend N50°W and are approximately 5 km. in length. The illumination azimuths

of the SIR-A and Seasat (60° and 62°, respectively) are such that the features are enhanced. Conversely, because the Landsat solar illumination azimuth is only 19°, the linear features are more nearly parallel to the direction of solar illumination, thus enhancement or detectability of these features decreases. Only the larger lineaments are obvious on the Landsat image. In this situation, the SIR-A imagery nicely complements the Landsat scene, and thus allows for a more comprehensive geologic analysis.

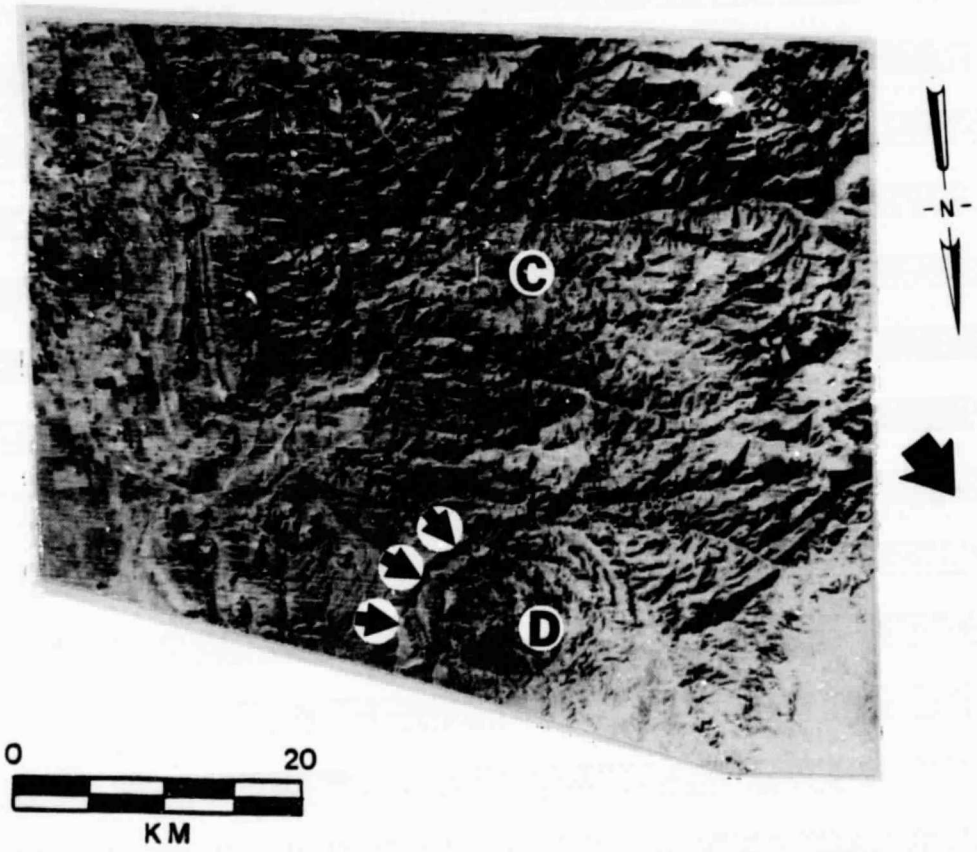

Figure 2. Landsat MSS image, band 7. Solar elevation 20°, solar azimuth 149° (indicated by arrow), ID No. 2690-16500.

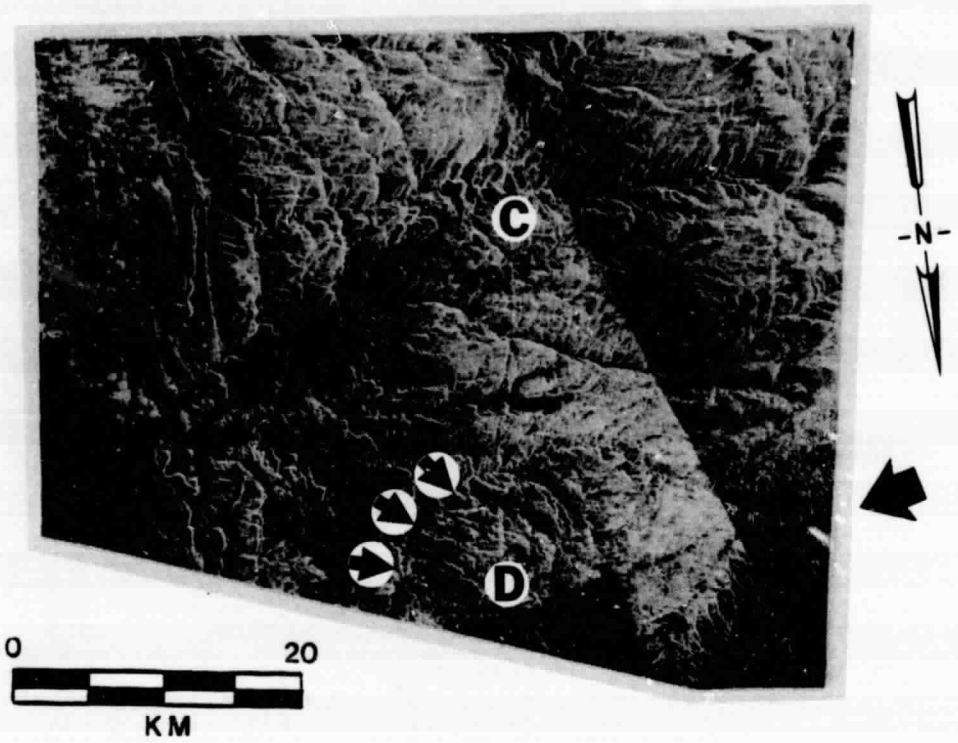

Figure 3. Seasat image, Rev. 580, look-direction indicated by arrow.

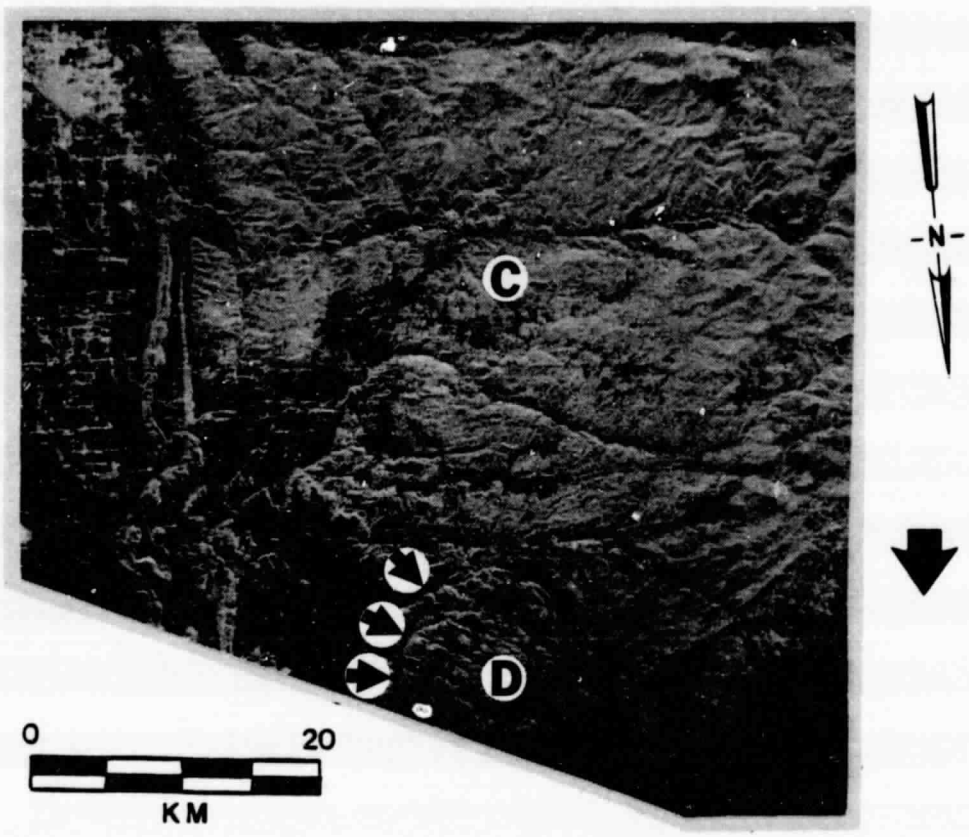

Figure 4. SIR-A image Orbit No. 20, look-direction indicated by arrow.

SECTION 3 COMPARISON OF SHUTTLE SIR-A RADAR IMAGERY AND AIRCRAFT RADAR IMAGERY FROM EASTERN PANAMA

Darien Province Area

SIR-A imagery illustrated in this section is from Panama and Darien Provinces in east-central and eastern Panama (Fig. 1). The climate is tropical, with the vegetation canopy continuous and the terrain marked by extremes of inaccessibility. Roads do not exist in most of the region; even the Pan American Highway has not been constructed through this part of Panama. Obtaining Landsat imagery or photography for geologic mapping in Darien Province has met with minimal success because of the almost perpetual cloud cover. This part of Central America serves adequately as an area typical of the tropical, cloudy environments with dense vegetal cover, characteristic of many countries in equatorial latitudes where adequate geologic mapping is lacking.

The Rio Turia flows around an isolated anticline (N on Figure 2A) which may be genetically related to a fold belt of north trending en echelon anticlines (K to L, Fig. 2A). Although there have been no significant oil or gas discoveries in this part of Panama to date, these anticlinal features represent classic examples of the landform expression of geologic structures commonly associated with hydrocarbon accumulation. Figure 3A is the product of a Ka-band aircraft system which acquired complete coverage of eastern Panama during 1967-1968. Structural axes and lineaments inferred from SIR-A (Fig. 2B,C) and aircraft radar (Fig 3B,C) are provided for comparison purposes.

Figure 1. SIR-A index map for eastern Panama.

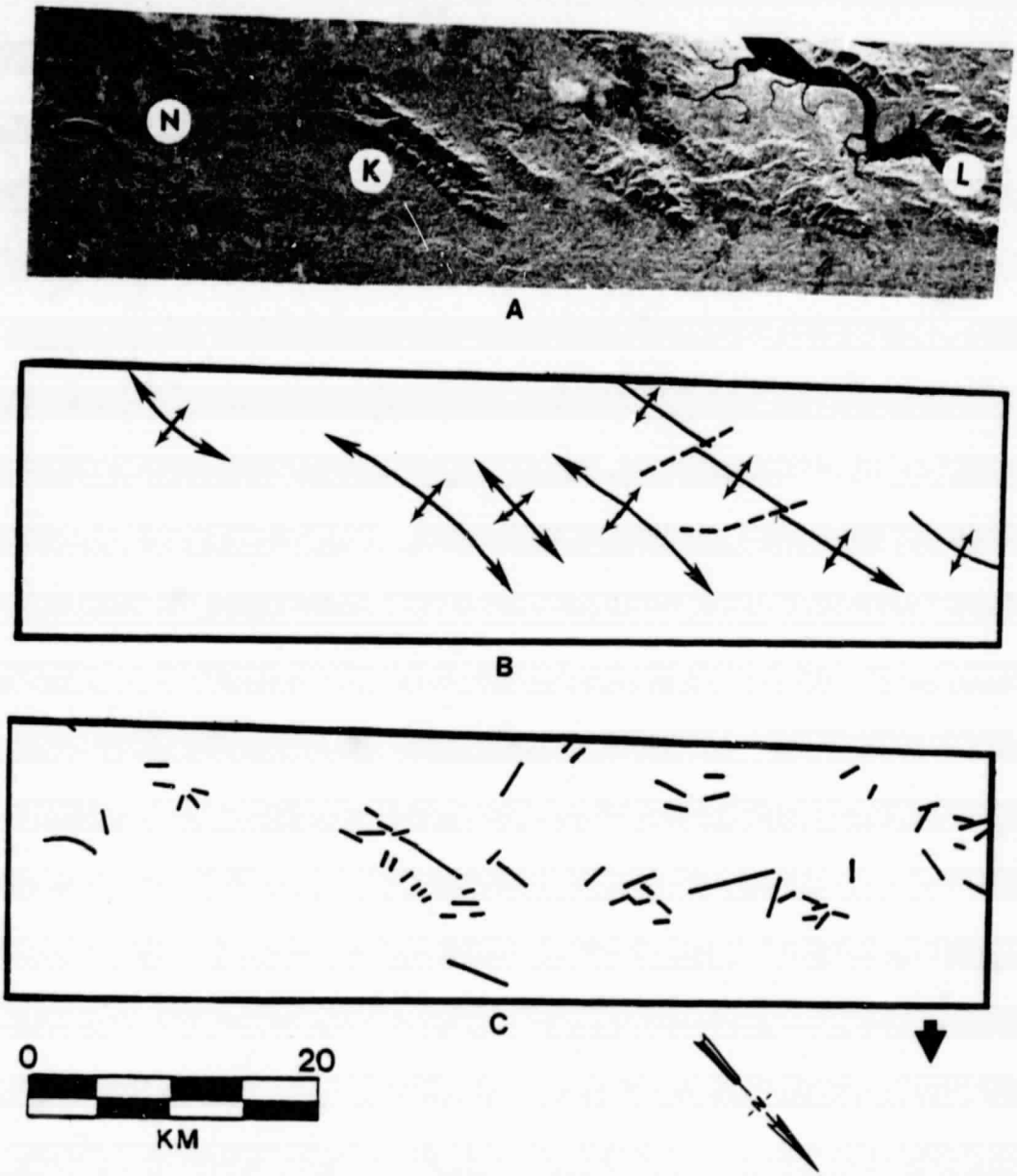

Figure 2. (A) SIR-A image taken from orbit 22, data take 24C.
(B) Structure map constructed from the SIR-A image.
(C) Lineament map constructed from the SIR-A image.
Look-direction indicated by arrow.

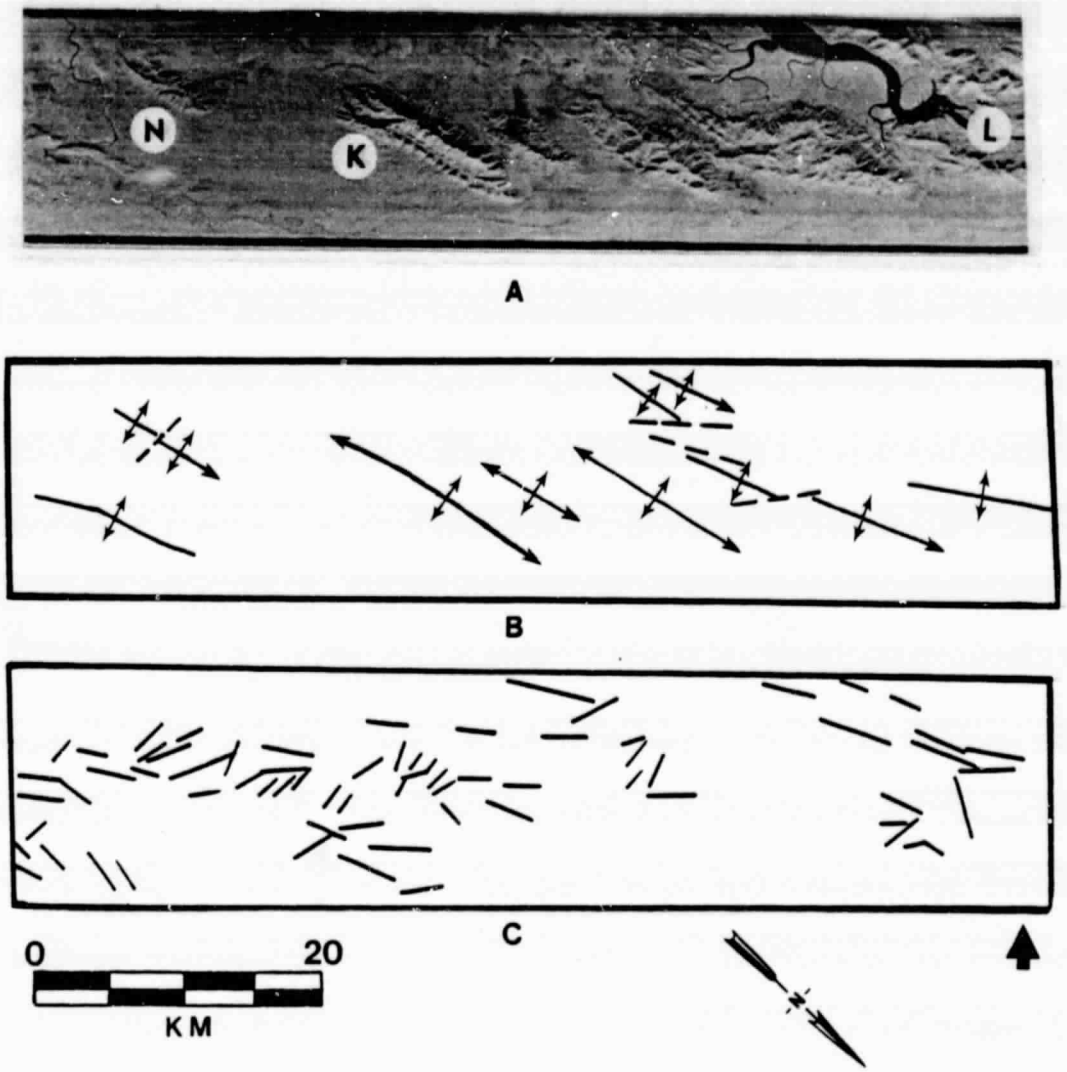

Figure 3. (A) Westinghouse AN/APQ-97 SLAR image. (B) Structure map constructed from the SLAR image. (C) Lineament map constructed from the SLAR image. Look-direction indicated by arrow.

A major part of the aircraft image (Fig. 3A) includes look-angles larger than those of SIR-A (47°±3°). Although similar major structures were mapped from both data sets, the more shallow illumination angle (larger look-angle) provided by the aircraft radar allows for the enhancement of subtle landform features resulting in an improved interpretation product. This aspect is especially evident on the Ka-band image (Fig. 4A), between points (Q) and (S) where several steeply dipping, thinly-bedded rock units are expressed as distinctive flatirons on the northeastern flank of the anticline. These same features are not well defined on the Shuttle SIR-A imagery (Fig. 4B).

The significant difference in geologic interpretability of Figures 5A and B is related primarily to the contrast in the range of look-angles for the two imaging systems. The subtle expression of terrain textures that are indicative of lithologic differences, are obvious on the aircraft image (Figure 5A, vicinity of area a-d). The same region is featureless on the SIR-A image (Fig. 5B). The evidence to support the importance of look-angle when comparing Figures 5A and 5B might be questioned because the images were obtained from two different (orthogonal) look-directions. However, Figures 6A and 6B contrast aircraft and SIR-A imagery obtained from the same look-direction. Landform portrayal of even the larger or more extensive features is significantly better on the aircraft radar imagery (Fig. 6A).

Unlike the impact of look-angle on geologic interpretation, the relatively better resolution of the Ka-band radar (15 m) as contrasted with the SIR-A radar (40 m) does not appear to significantly influence geologic

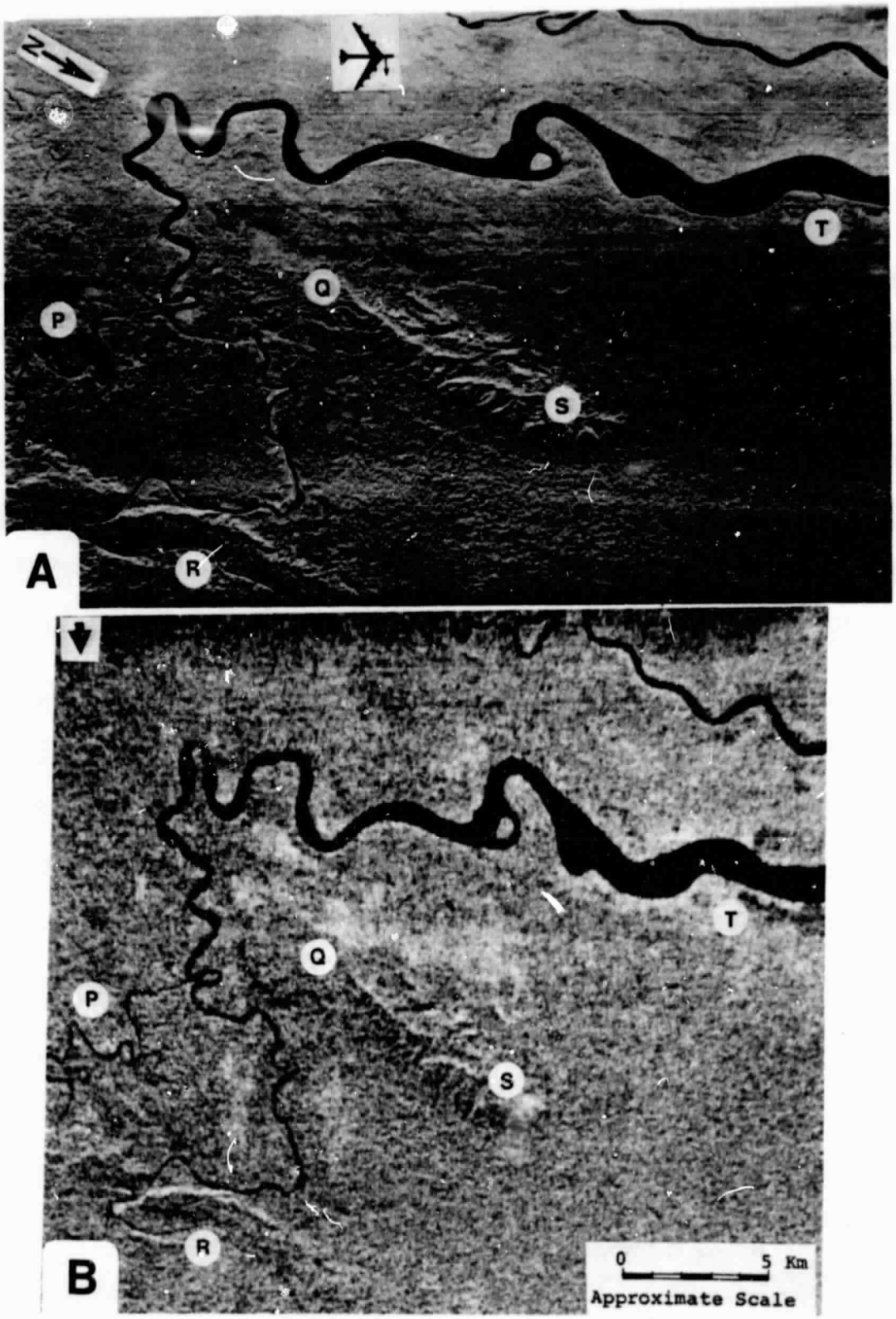

Figure 4. (A) Ka-band aircraft imagery, (B) Enlargement of SIR-A imagery orbit 22 data take 24C.

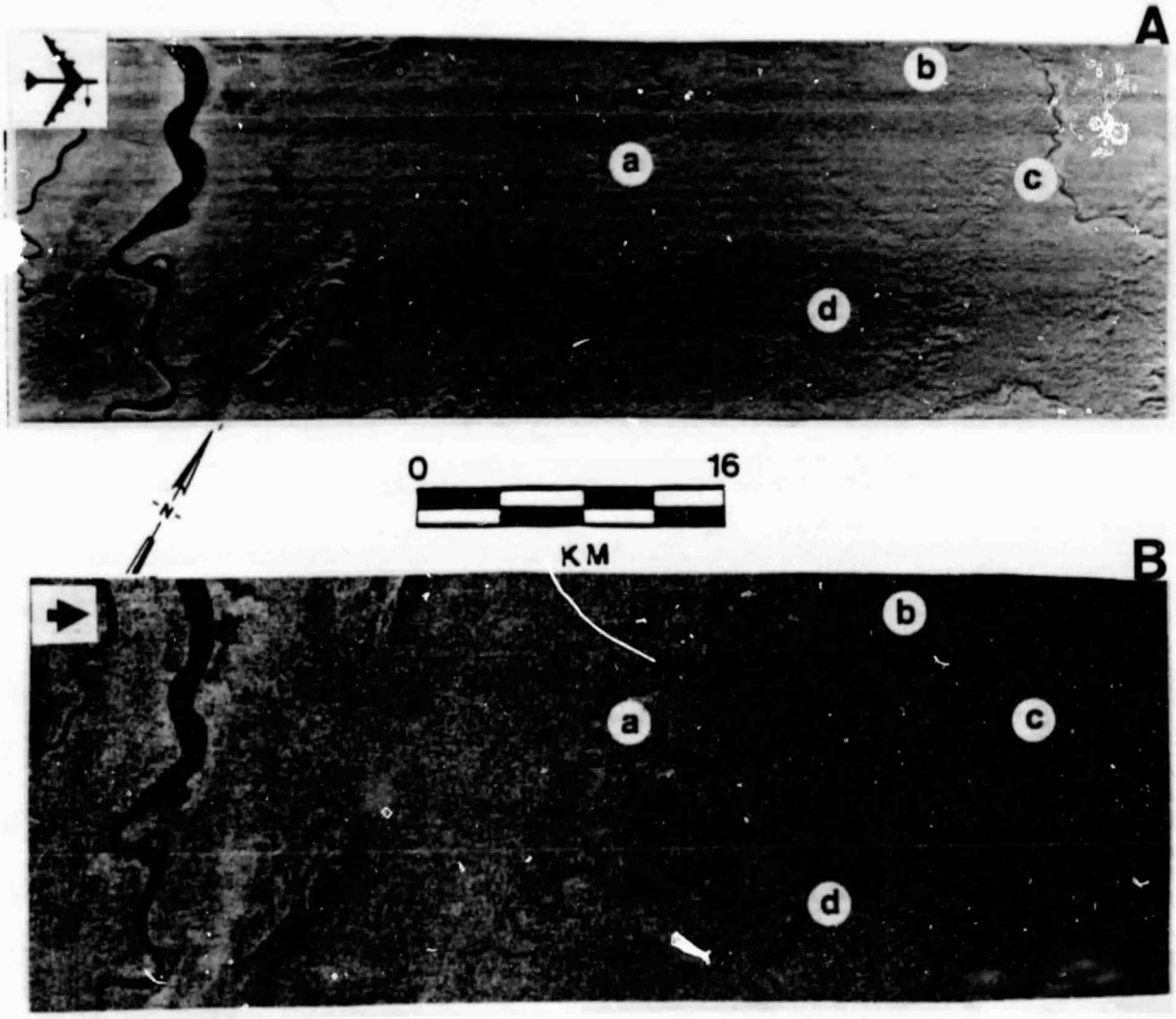

Figure 5. (A) Ka-band aircraft imagery, (B) SIR-A imagery. Orbit 22, data take 24C.

reconnaissance mapping, i.e. recognition and detection of gross landform features. However, smaller streams with narrow channels which were detectable on the aircraft imagery were not obvious on the Shuttle radar. See for example, the small streams entering the Rio Turia especially in the vicinity of areas a, b, and c, Figures 5A and 5B.

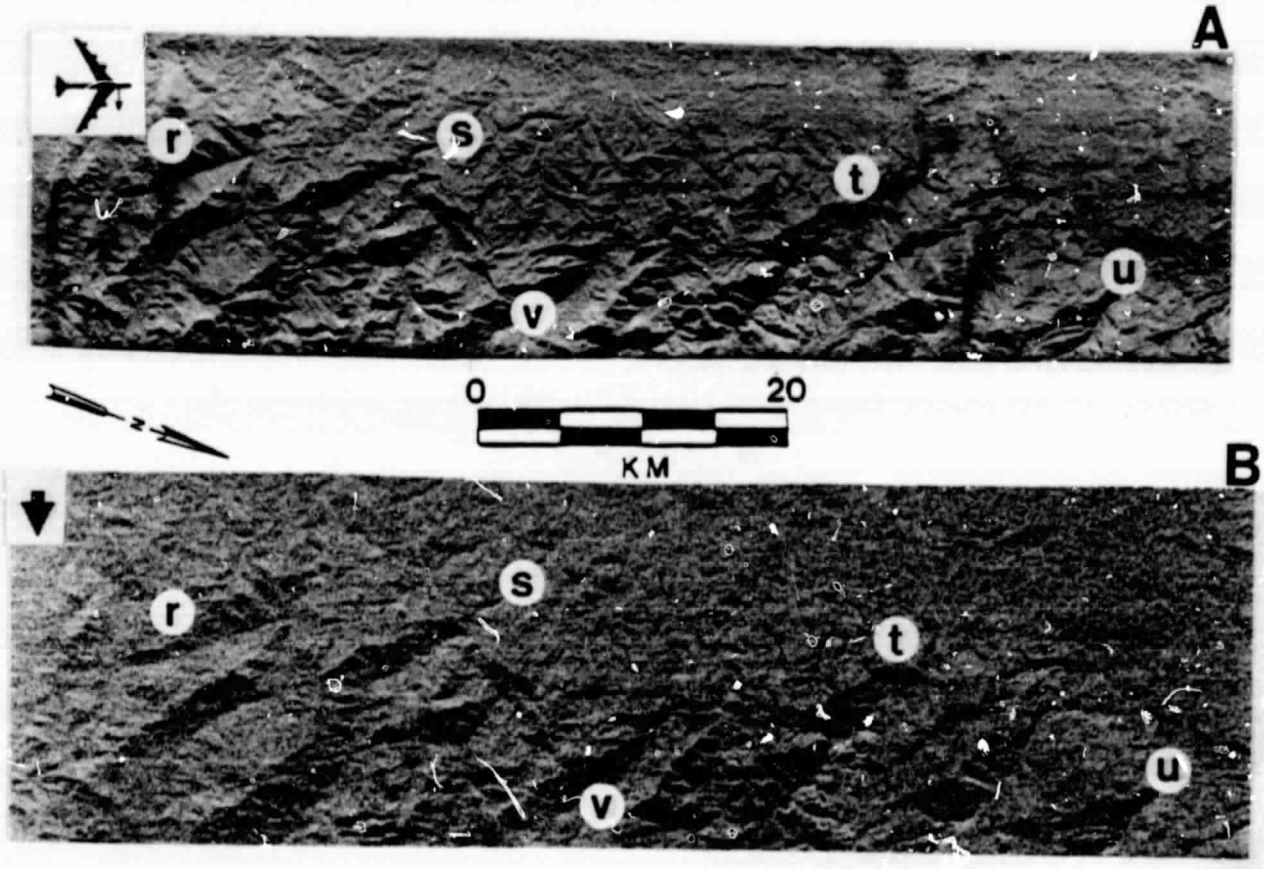

Figure 6. (A) Ka-band aircraft imagery, (B) SIR-A imagery. Orbit 22, data take 24C.

Bayano Reservoir, Panama

SIR-A imagery including coverage of the Bayano Reservoir (Figure 7) was of considerable interest to hydrologists of Panama's Institute of Hydrometerology Resources and Electrification (IHRE). Primarily, because of the lack of accurate maps, aerial photographs, or Landsat imagery (near perpetual cloud cover), the radar imagery provided the first estimate of the reservoir's areal extent since initial impoundment of the Bayano River in 1976. Of secondary importance to the Panamanians (but of considerable interest to our SIR-A investigations) were the causes of anomalous radar returns recorded on the SIR-A imagery in the eastern part of the reservoir (Fig. 7, areas A, B, C, and D). These tonal signatures varying from white to mottled black, contrast significantly from the uniform gray tones characteristic of the surrounding jungle canopy. Figure 8 provides a pre-flood (1968) rendition of the terrain configuration as recorded by a Ka-band aircraft radar imaging system of nearly the same area.

MacDonald, et al. (1980), Waite, et al. (1981), and Krohn, et al. (1983) have demonstrated that the Seasat imaging radar was particularly sensitive to contrasting terrain differences. Especially in the wetland environment, the presence of standing water beneath a vegetation canopy radically altered the radar scattering characteristics. The authors also suggested that definition of anomalous radar tonal signatures in wetland terrain could lead to improved discrimination of vegetation classes and improved estimates of biomass. Although the look-angles of Seast ($20°\pm3°$) and SIR-A ($47°\pm3°$) were markedly different, the anomalously bright radar

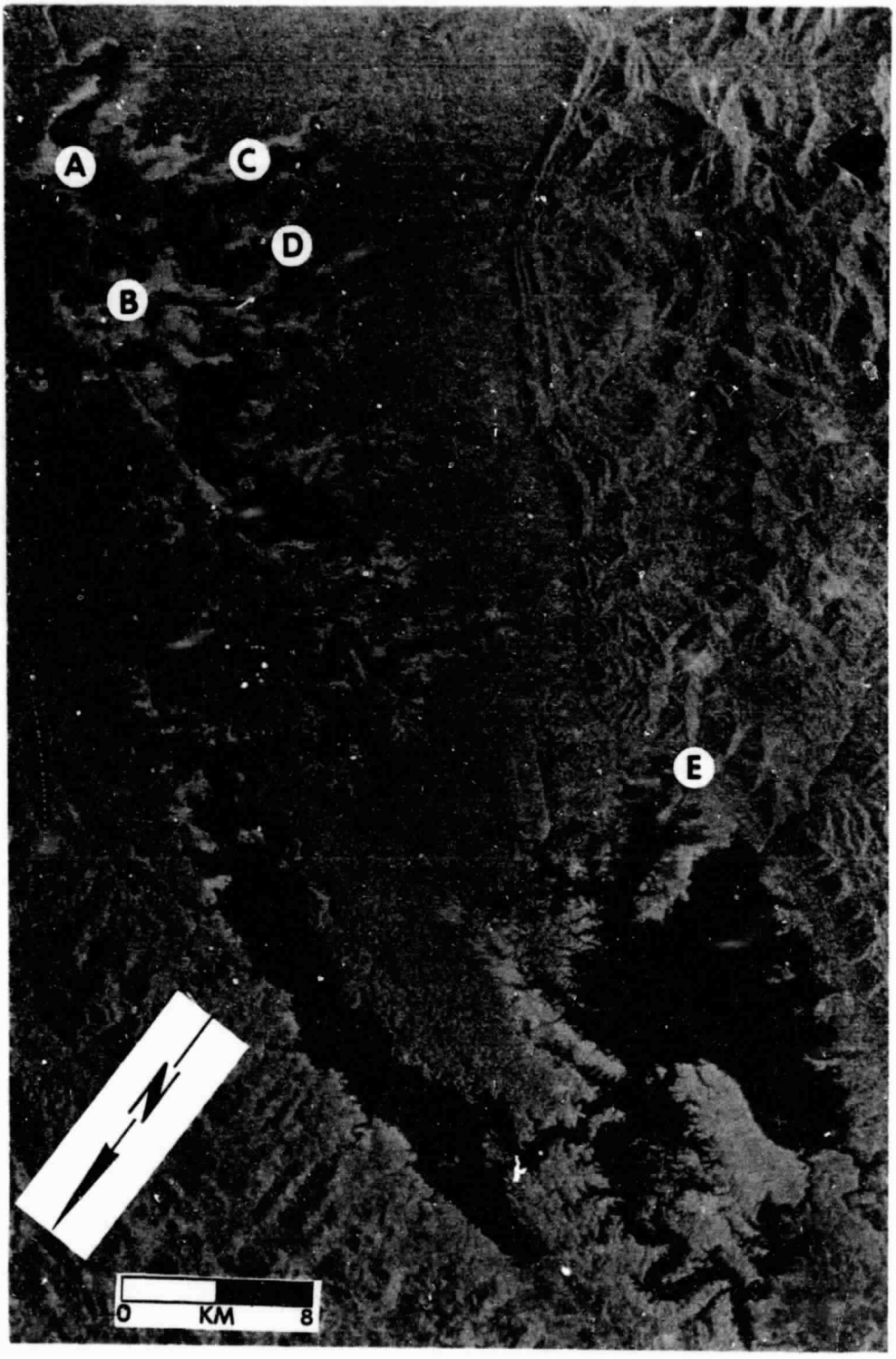

Figure 7. SIR-A imagery, Bayano Reservoir, Panama.

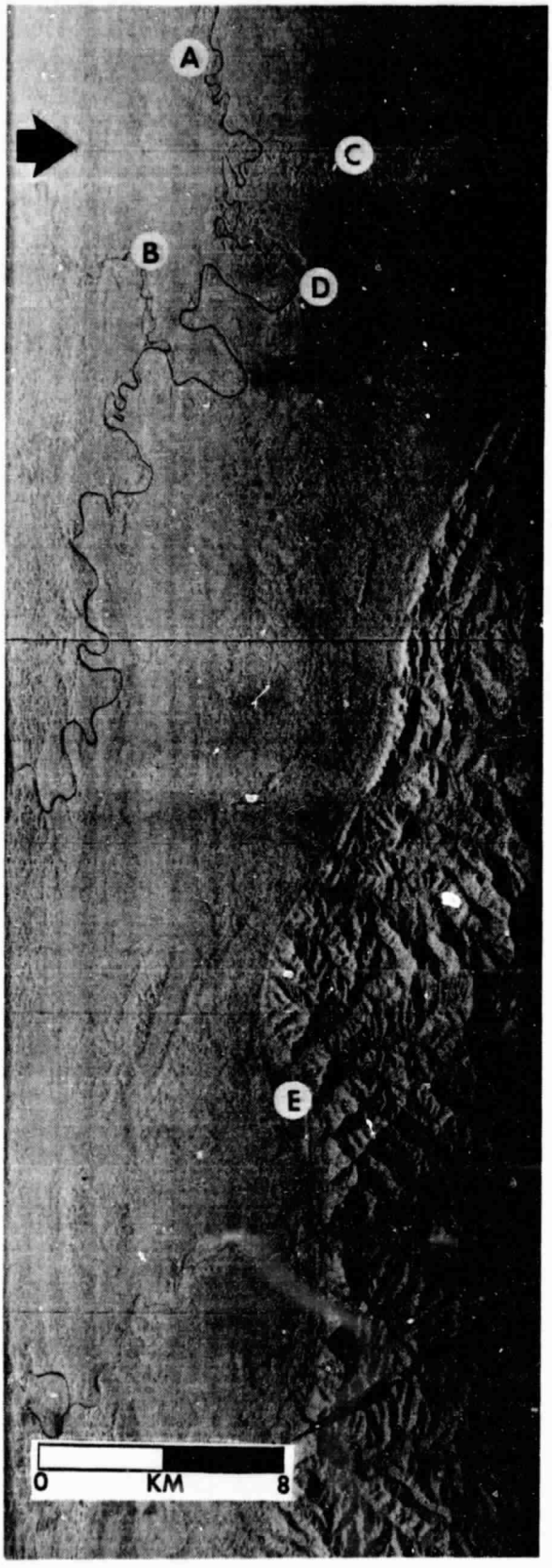

Figure 8. Ka-band Radar, Bayano River, pre-flood.

signatures recorded by both radar systems in wetland areas appeared to be somewhat similar. To help understand the origin of these radar signatures, field work was coordinated with the Panamanians. Ms. Claudia Candanedo, Director of IHRE kindly provided technical and logistical support during June 1983. Meetings with professional staff familiar with the Bayano Reservoir proved to be very helpful in assessing the terrain and vegetation characteristics of the area. From the outset one obstacle in determining the cause of the anomalous returns became apparent. At the time of imagery acquisition in November of 1981, the water level of the reservoir (above M.S.L.) stood at 60.23 m. At the time of ground truth studies in mid June 1983, the reservoir was at 51.53 m, the consequence of a year long draught in Panama. It was clear that field checking would not answer all the questions because the appearance of the reservoir would be quite different from that when the imagery was obtained. Fortuitously however, IHRE personnel had conducted field work near the time of the SIR-A orbit and numerous slides and photographs were made available.

Figures 9 and 10 provide location points on the SIR-A imagery that correspond with the ground scenes of Figures 11-14. The brightest image tones were correlated with areas covered with Cyperus luzulae. Cyperus is a heavy rice like plant that grows in uneven clumps approaching one meter in height. Figure 11 is an area of open water and rafts of Cyperus. This photograph was taken from the open water (dark) and looks shoreward toward an area of Cyperus and dead trees (bright).

The dark-mottled tonal signatures on the SIR-A imagery (Figure 10, location 6) has been correlated with areas of aquatic Pistia stratiotes.

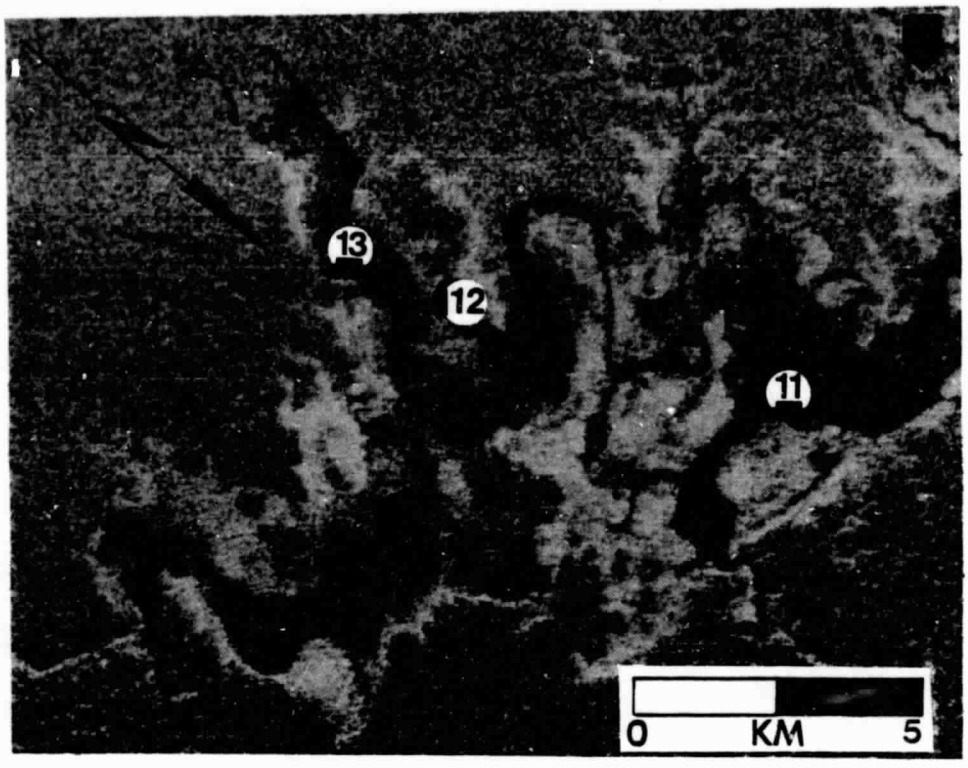

Figure 9. SIR-A of eastern Bayano Reservoir. Location of ground scenes, Figures 11, 12, and 13.

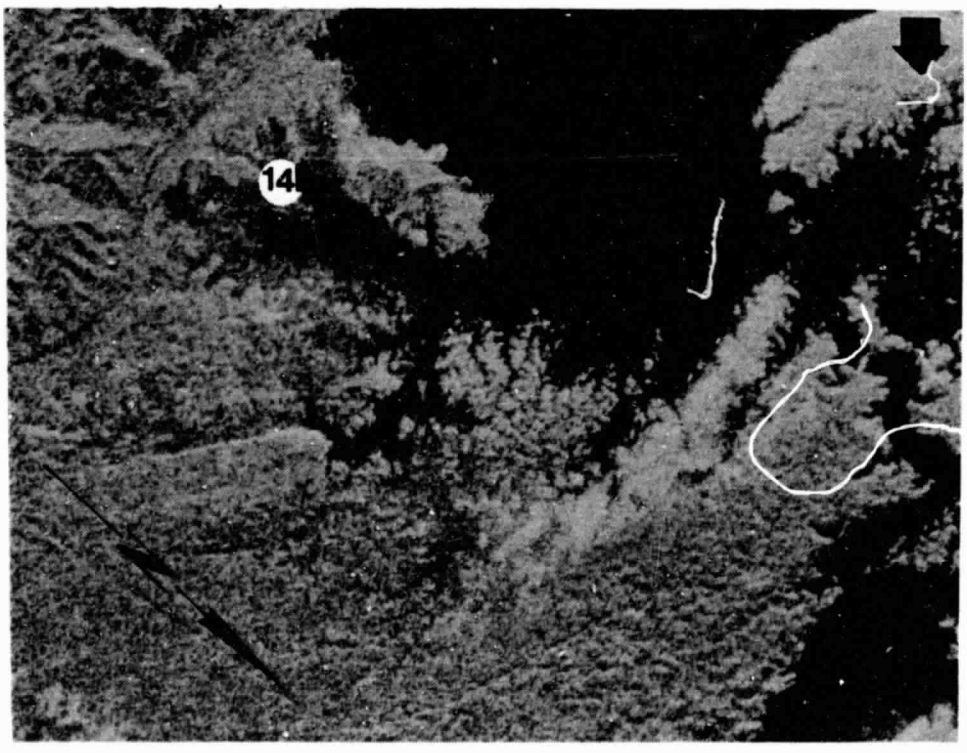

Figure 10. SIR-A image of western Bayano Reservoir. Location of ground scene, Figure 14.

Pistia is a flat-lying floating plant that forms a dense, relatively smooth "carpet" on the water surface (Fig. 12).

Figure 13 provides a ground scene of both the low lying Pistia (foreground) and the taller Cyperus (background). Cyperus grows in shallower water (<8 m depth) than Pistia, and tends to grow among the trunks of the dead trees near shore. The influence of the tree trunks on the bright radar signature from Cyperus areas is being investigated.

Areas within the Bayano Reservoir having an intermediate gray tone between Cyperus (white) and Pistia (mottled black) can usually be correlated with mixtures of the two interspersed with various taller aquatic grasses and plants. Figure 14 illustrates a combination of Pistia and other various aquatic grasses and plants.

Figure 11. Bayano Reservoir, November 1981. Rafts of Cyperus.

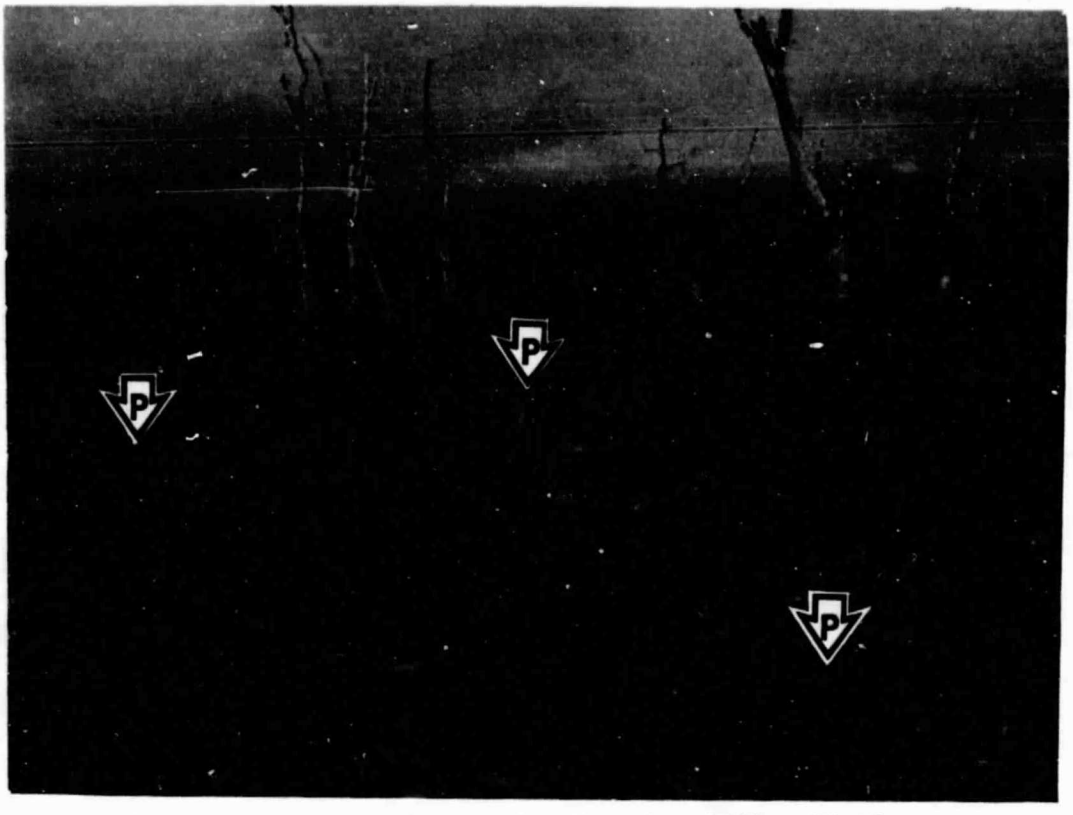

Figure 12. Bayano Reservoir, November 1981. Pistia.

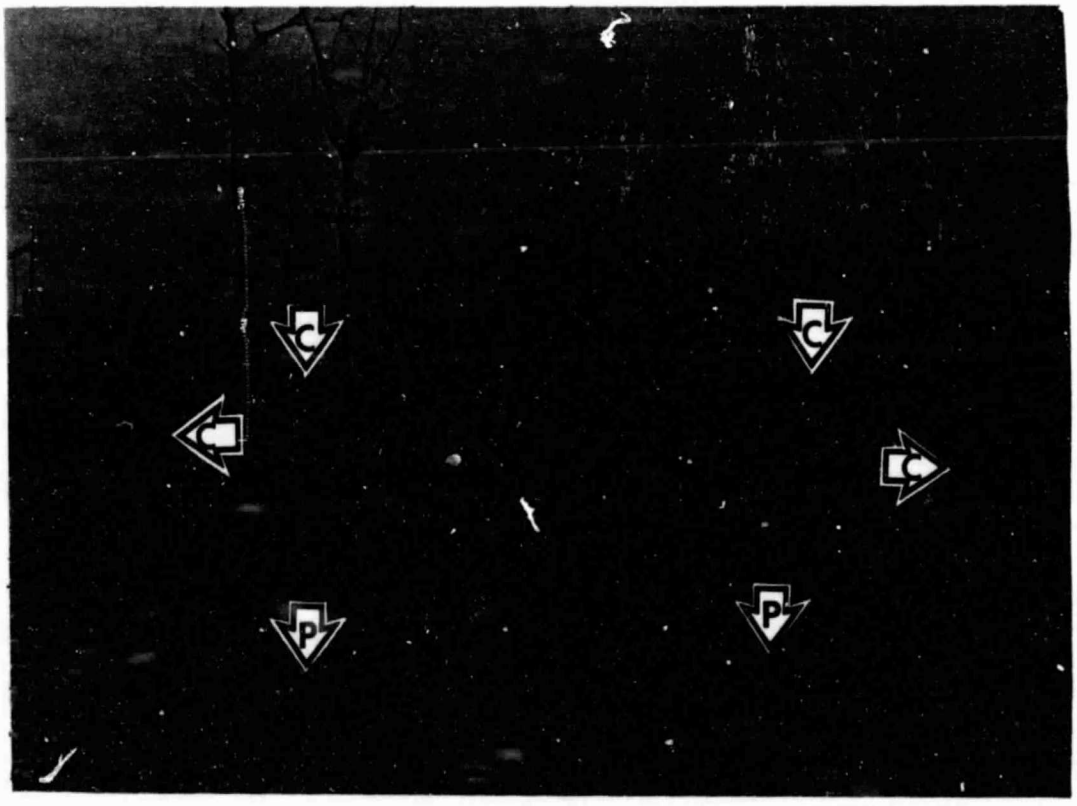

Figure 13. Bayano Reservoir, November 1981. Pistia and Cyperus.

Figure 14. Western part of Bayano Reservoir, November 1981. Pistia and other aquatic grasses and plants.

REFERENCES SECTION 3

Krohn, D.M., N.M. Milton, and D.B. Segal, 1983, Seasat Synthetic Aperture Radar (SAR) Response to Lowland Vegetation Types in Eastern Maryland and Virginia: Jour. Geophysical Res., vol. 88, no. C3, p. 1937-1952.

MacDonald, H.C., W.P. Waite, and J.S. Demarcke, 1980, Use of Seasat Satellite Radar Imagery for the Detection of Standing Water Beneath Forest Vegetation: Proc. Amer. Soc. Photogramm., Fall Tech. Mtgs., Niagara Falls, NY, October, 1980, p. RS-3-B-1 to RS-3-B-13.

Waite, W.P., H.C. MacDonald, V.H. Kaupp, and J.S. Demarcke, 1981, Wetland Mapping with Imaging Radars: International Geoscience and Remote Sensing Symposium (IGARSS'81) Digest, vol. 2, p. 794-799, June 1981.

SECTION 4 COLOMBIAN ANDES

Location

The study area encompasses 2500 km^2 centered at 6°50'N and 76°10'W. The area is defined by the intersection of SIR-A data takes 24C and 10-11 (Fig. 1). The structure of the Western Andes is dominated by large thrust and left lateral strike slip faults that have been mapped along the entire length of the Colombian Andes. Along the shuttle track to the south on data take 24C, these faults are within 10 km of the study area. The Romeral, Sabanalargo, and Santa Rita faults trend due north to N10°W (Fig. 2). An enlargement of the geologic map of the study area is provided in Figure 3. Two SIR-A images, one Landsat band 6 scene (0.7-0.8 micrometers), and a Ka-band (0.86 cm wavelength) radar were available for this study area.

Lithologic Mapping

In regions where broad expanses of rock are exposed and/or are close- reflected in the terrain configuration, generalized rock types and regional facies changes in major sedimentary units might be mapped from evidence presented on a radar data format. However, in those areas having the combination of low relief and heavy vegetation or mantle cover, or in areas having poorly exposed rock units, diagnostic or suggestive lithic criteria may be completely absent.

The rugged terrain of the Colombian Andes provides a perfect example of an area masked by heavy vegetation and where lithologic inference is

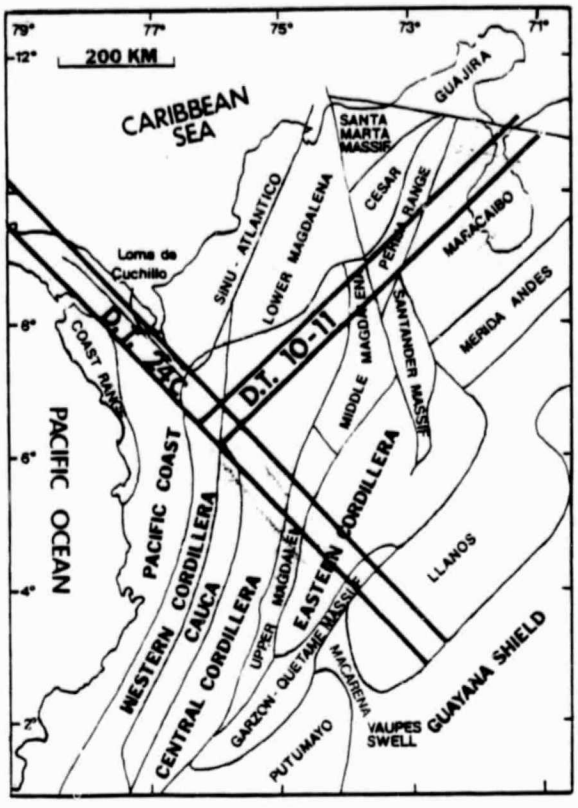

Figure 1. Location map of study area.

extremely difficult because of the lack of distinctive landforms. However, terrain textural variations that may be indicative of lithologic boundaries can be recognized within areas A, B, and D, Figures 4, 5, and 6. The somewhat smooth texture of areas A, B, and D may be related to a fine-grained rock type surrounded by a relatively coarse-grained volcanic sequence. Subtle evidence of stratification is provided by north-trending linears in area C Figure 4.

Area E (Fig. 4) is a large domal feature that exhibits annular drainage. No change in drainage density or tone from the surrounding area is evident. However, the shape may be caused by an underlying basalt plug

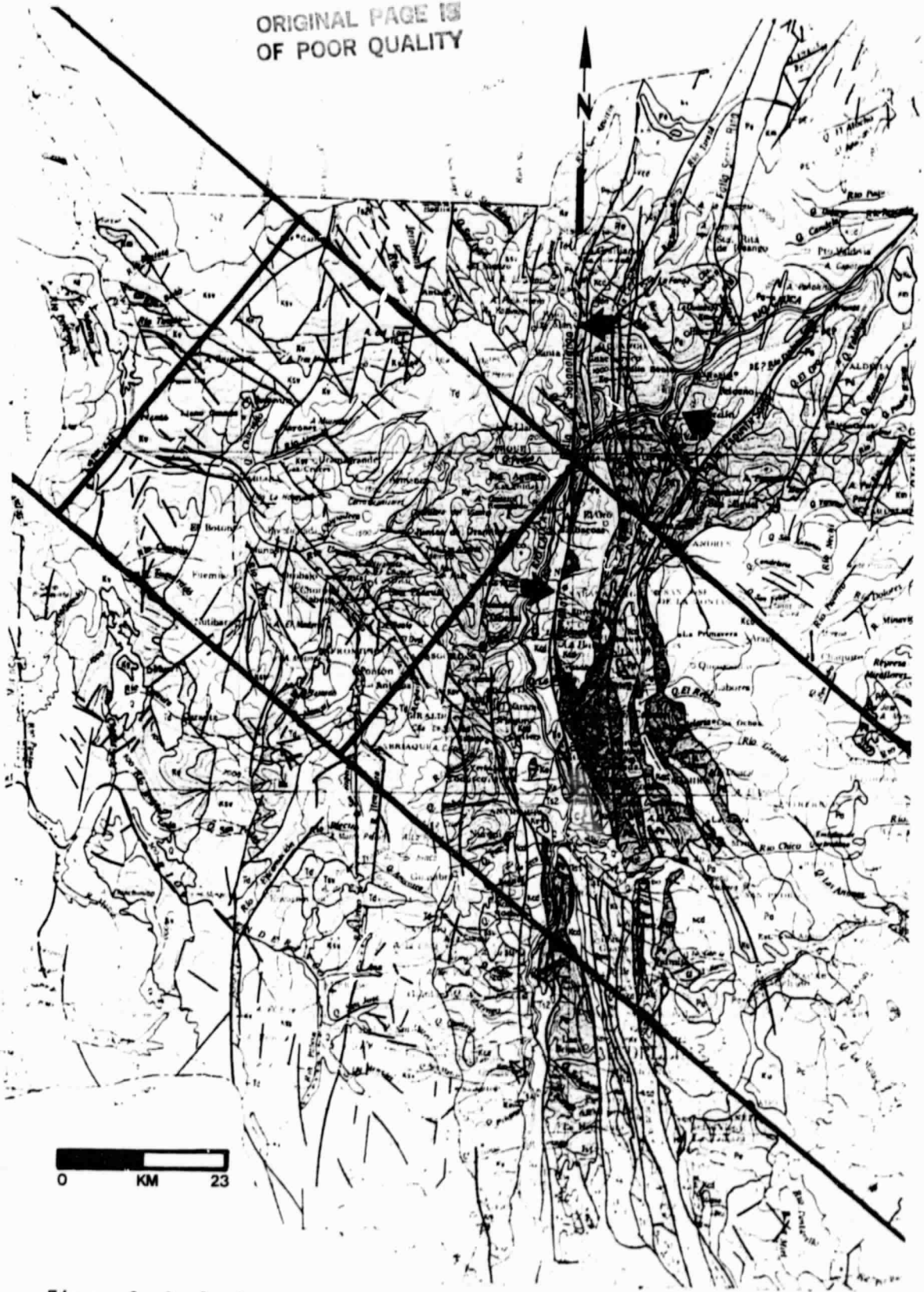

Figure 2. Geologic map of study area vicinity.

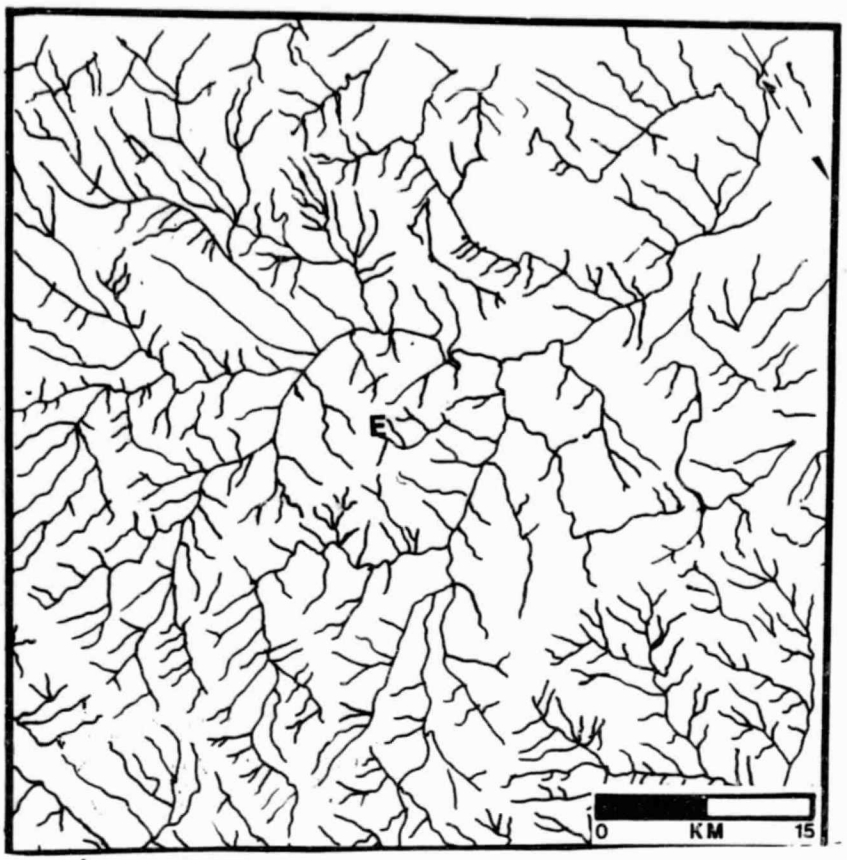

Figure 9. Drainage map interpreted from Figure 7.

direction resulting in reduced solar highlighting and shadowing. SIR-A drainage mapping can be shown to be a significant improvement over the drainage patterns inferred from Landsat (Fig. 12). Especially in the vicinity northeast of area E (Fig. 12), neither of the SIR-A drainage maps (Figs. 9 and 10) allows for increased river and tributary discrimination.

or ultramafic rock. In Brazil, domes such as these have been mapped as ultramafic units with a weathered nickle laterite cap (Allum, 1981). Field checking would be required to verify any of these observations.

The advantage of SIR-A type radar imagery over that obtained from aircraft is particularly evident when comparing Figures 4 and 6. The Ka-band radar mosaic (Fig. 6) was constructed from four opposite-look flight lines (flown approximately west to east and east to west), and the far range of each image contains extensive radar shadowing. Although foreshortening and layover are less severe on the aircraft imagery than on the SIR-A data, radar shadow is a considerable disadvantage on the interpreter.

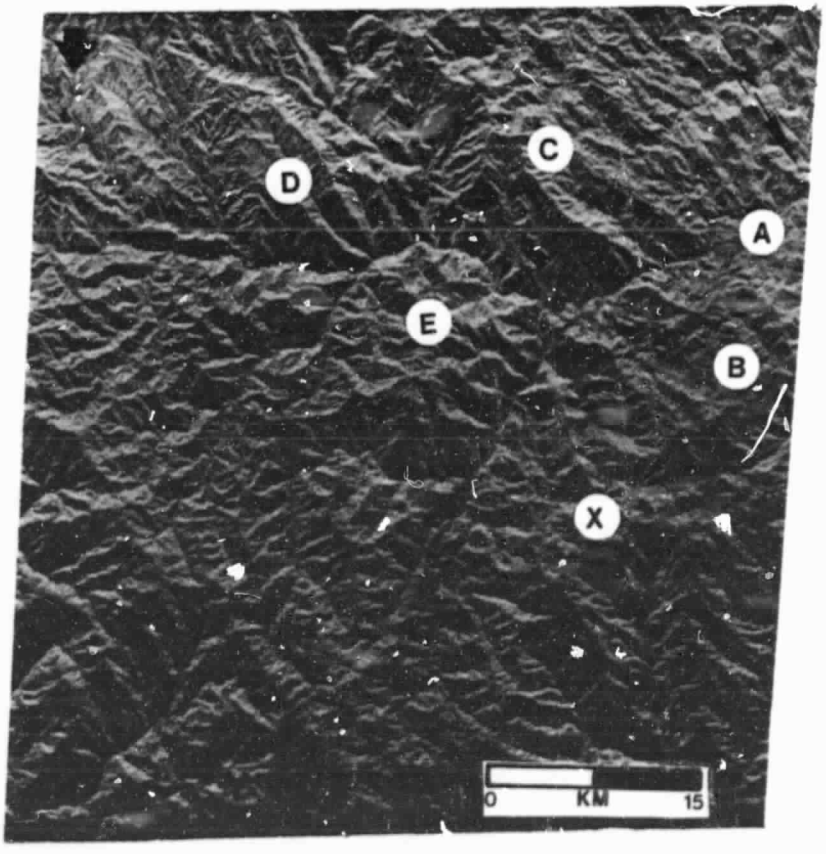

Figure 4. SIR-A data take 24C.

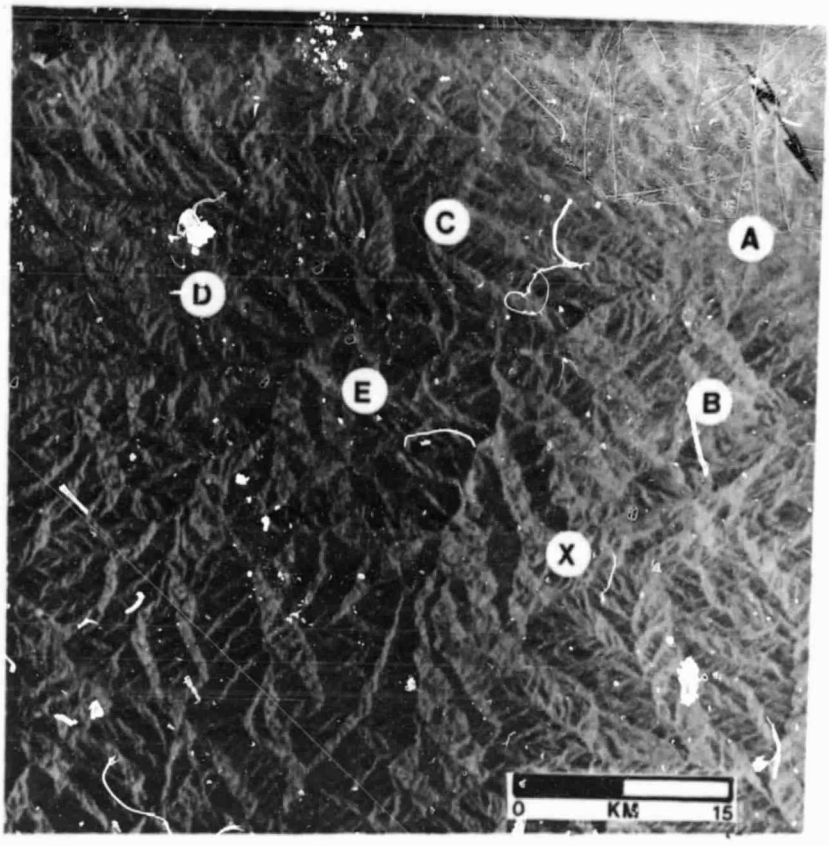

Figure 5. SIR-A data take 10-11.

Drainage Mapping

The orientation of a landform relative to the look-direction of an imaging radar system (referred to in Section 2 of this report as illumination azimuth) has a considerable effect on the way radar portrays that landform. A stream valley with valley walls parallel to radar look-direction (small illumination azimuth angle) will be suppressed on a radar image. This is because the angle of incidence of the radar beam is equal on both walls of the stream valley, resulting in equal power returns from both valley walls. Consequently, equivalent power returns appear as the same gray tone on a radar image. This lack of contrast from opposing

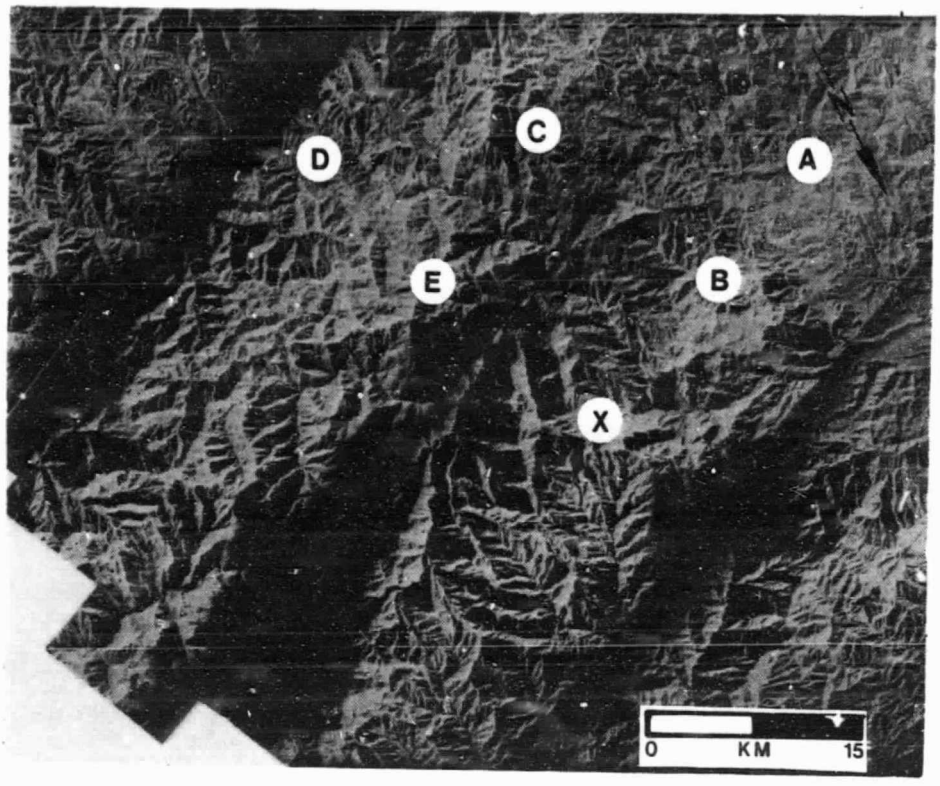

Figure 6. Ka-band radar mosaic.

valley slopes makes recognition of the stream valley difficult. This effect can be seen by comparing streams 2, 3, 5, and 7 on Figures 7 and 8. The converse is true for a stream valley oriented near perpendicular to the impinging radar beam (relatively large illumination azimuth). Because of highlighting and shadowing, opposing walls can return significantly different amounts of radar energy. The enhancement of stream valleys can be seen by comparing streams 1, 4, and 6 on Figure 7 with their counterparts on Figure 8.

In addition to marked differences in highlighting and shadowing of similar landforms when imaging high slope/relief terrain from opposite

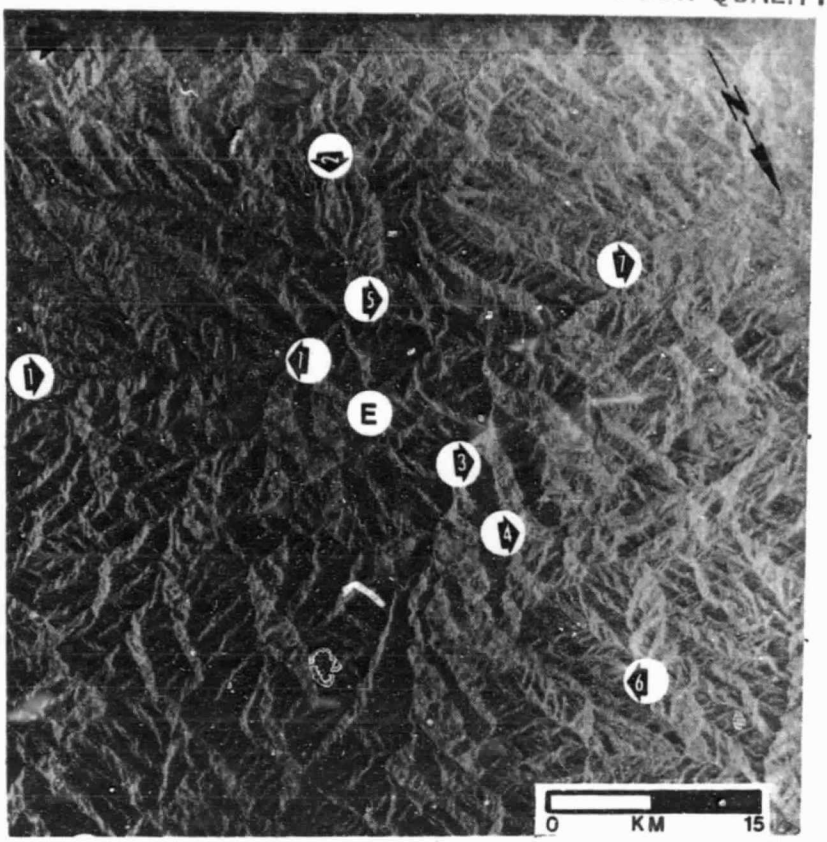

Figure 7. SIR-A data take 10-11

or orthogonal look-directions, geometric distortions (foreshortening and layover) in the image formats can be considerable. These distortions influence the interpretability of the image and are reflected in the map products. Visual comparison of the northeastern quadrant (lower left) of Figures 7 and 8 allows for comparisons of rugged terrain imaged from orthogonal look-directions. The contrasting terrain appearance is reflected in the mapped drainage patterns (Figs. 9 and 10) from these two space radar images. Differences in the mapped drainage patterns are also evident in the vicinity of area 7. The complementary advantage of two near-orthogonal look-directions for drainage mapping is obvious in this

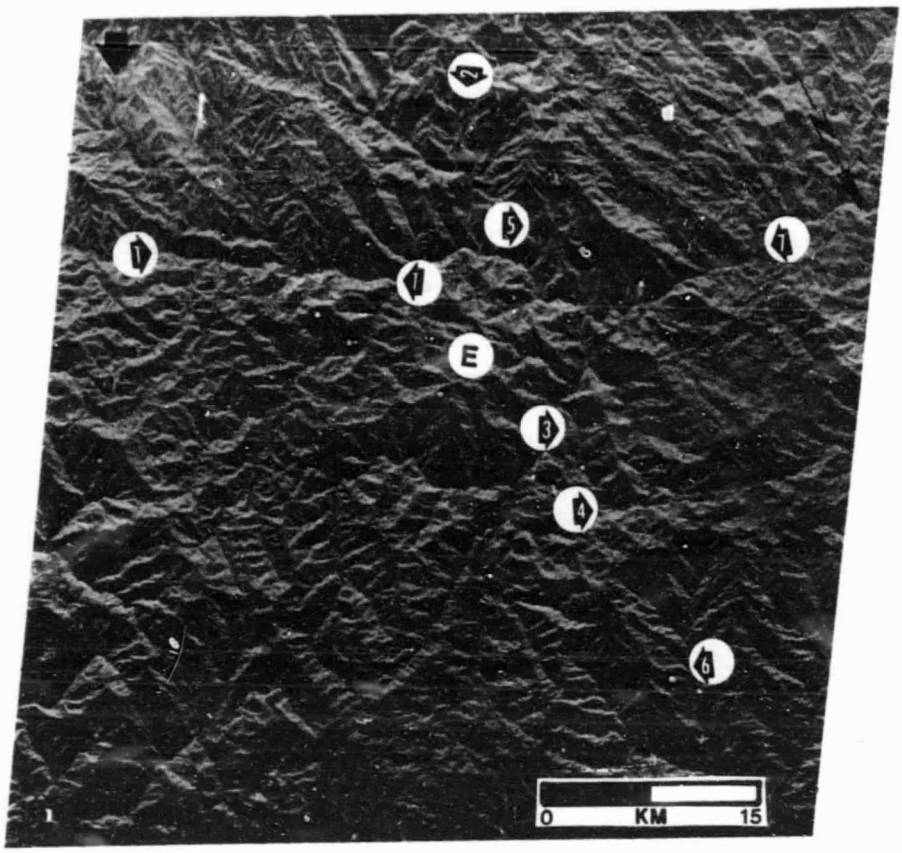

Figure 8. SIR-A data take 24C.

comparison.

The best available (relatively cloud free, i.e. less than 30%) Landsat image of the study area is provided in Figure 11. While major river and tributary stream valleys having large illumination azimuth angles are well defined, smaller illumination azimuths result in reduced detectability of these same features. See for example, stream valleys at locations 1 and 4 which are poorly defined on the Landsat image (Fig. 11). The orientations of these valley walls are nearly parallel to the solar illumination

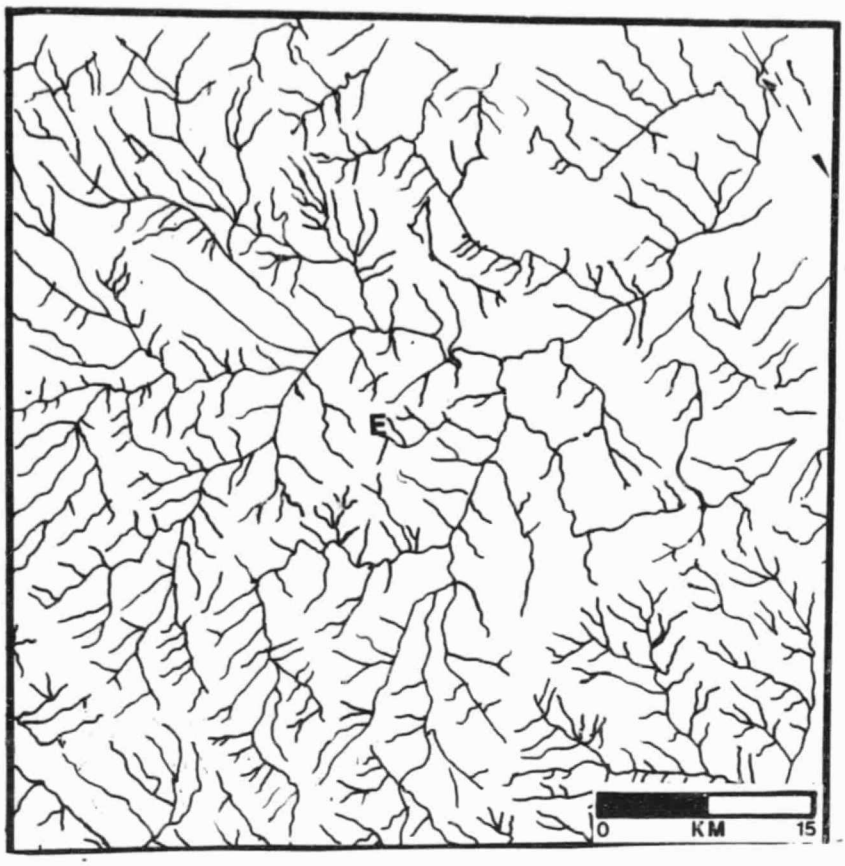

Figure 9. Drainage map interpreted from Figure 7.

direction resulting in reduced solar highlighting and shadowing. SIR-A drainage mapping can be shown to be a significant improvement over the drainage patterns inferred from Landsat (Fig. 12). Especially in the vicinity northeast of area E (Fig. 12), neither of the SIR-A drainage maps (Figs. 9 and 10) allows for increased river and tributary discrimination.

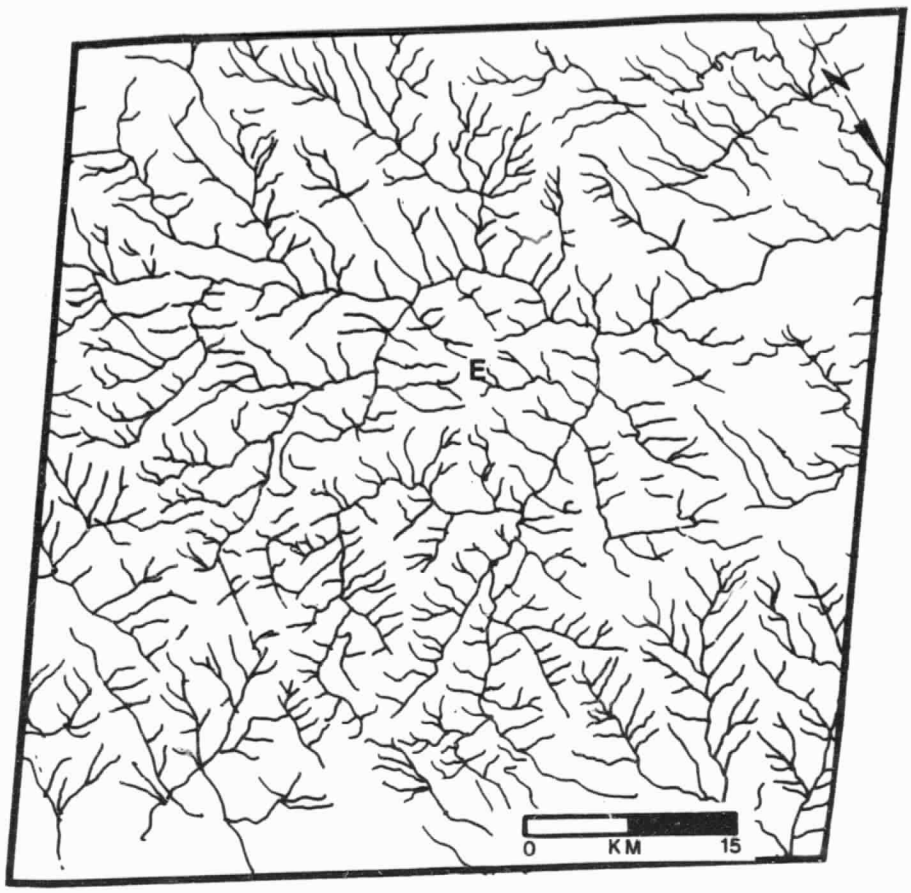

Figure 10. Drainage map interpreted from Figure 8.

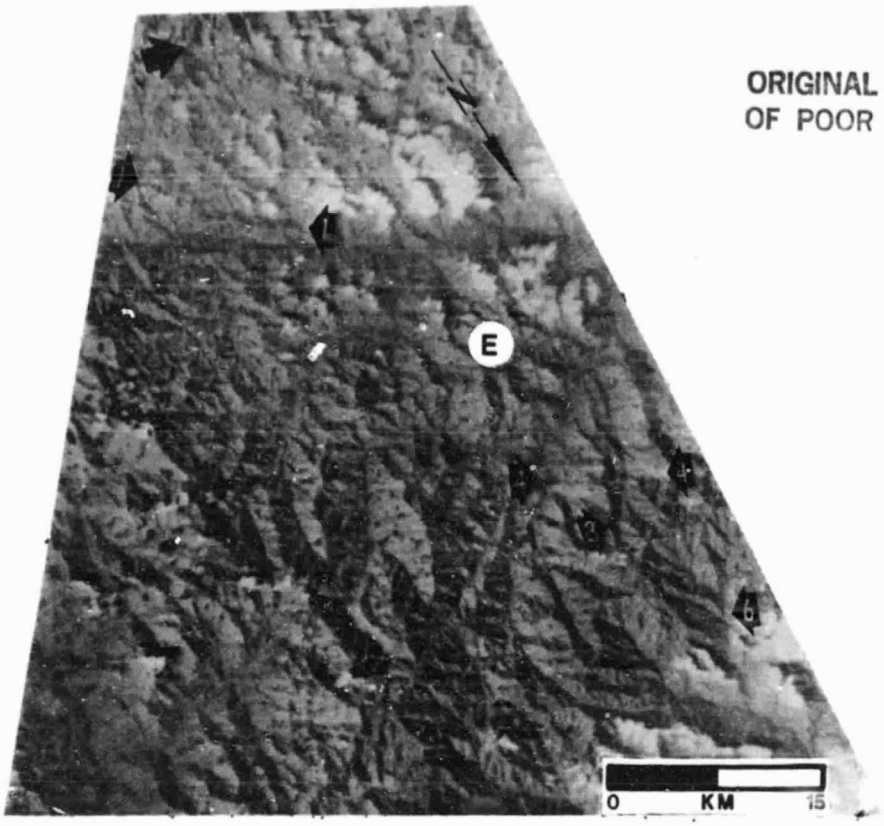

Figure 11. Landsat MSS band 6, solar elevation 44°, azimuth 99°, ID E-21149-14095-6.

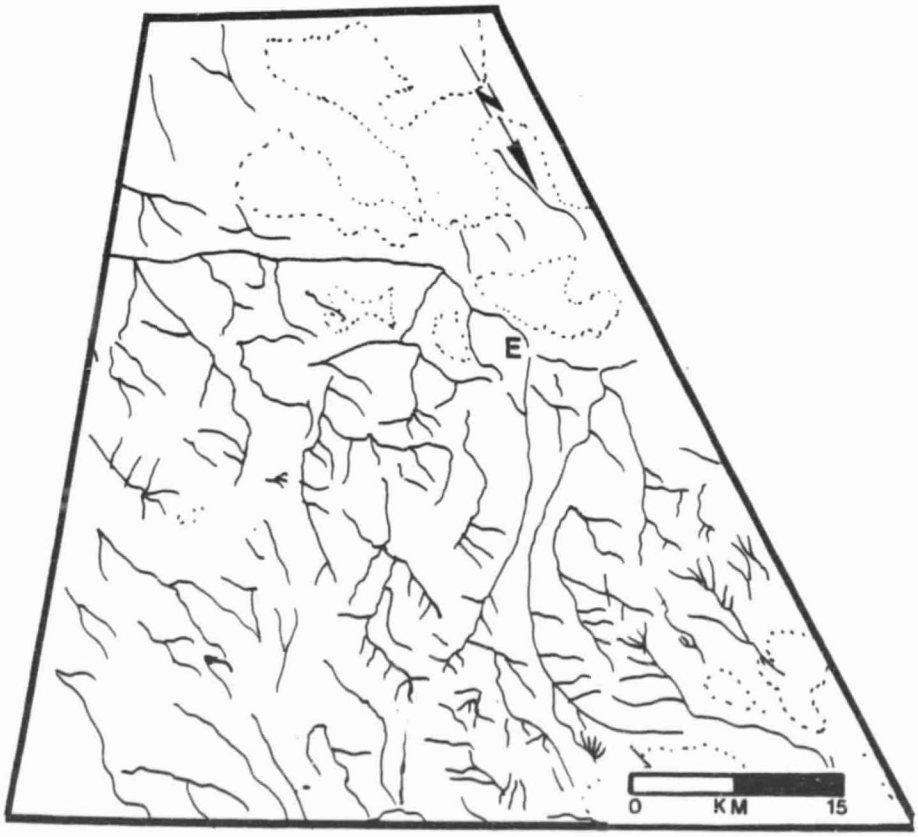

Figure 12. Drainage map interpreted from Figure 11.

Lineament Analysis

Similar to stream valleys, topographically expressed faults and other landform features can be enhanced or suppressed, depending on an imaging system's look-direction and consequent illumination azimutn. To demonstrate the importance of multiple look-directions over a single look-direction, lineaments were mapped from the two intersecting SIR-A orbits previously discussed (Fig. 1). All lineaments inferred from the SIR-A data were topographically expressed landform features.

SIR-A data takes 24C (Fig. 13A) and 10-11 (Fig. 14A) provide coverage of the same area, nearly orthogonal to one another. Interpretation of the SIR-A imagery with a northeast look-direction (Fig. 13A), resulted in a lineament map (Fig. 13B) and a length/orientation rosette diagram (Fig. 15). A similar interpretation was done for SIR-A imagery with a northwest look-direction (Fig. 14A), resulting in a lineament map (Fig. 14B) and a rosette diagram (Fig. 16).

Major differences between mapped lineaments (Figs. 13B and 14B) and rosette diagrams (Figs. 15 and 16) are related to contrasting look-directions and consequent image distortions (foreshortening and layover). Significantly, in this region of steep slopes and high relief, lineament mapping was less difficult when the look-direction of SIR-A was nearly parallel to the landform features and image distortion was minimized. For example, the north-trending linear stream valleys in the vicinity of area A Figure 13A, appear geometrically distorted on Figure 14A because of excessive relief displacement (layover). Comparison of Figures 15 and 16 provide evidence to support the need for multiple look-directions for optimum data retrieval. The complementary nature of data sets becomes obvious when the look-directions are near orthogonal.

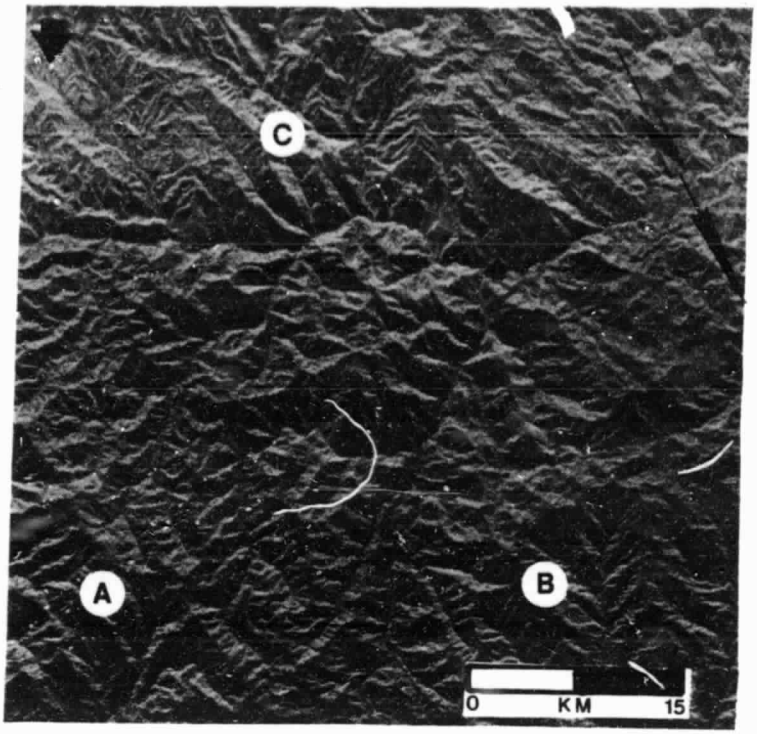

Figure 13A. SIR-A imagery, data take 24C.

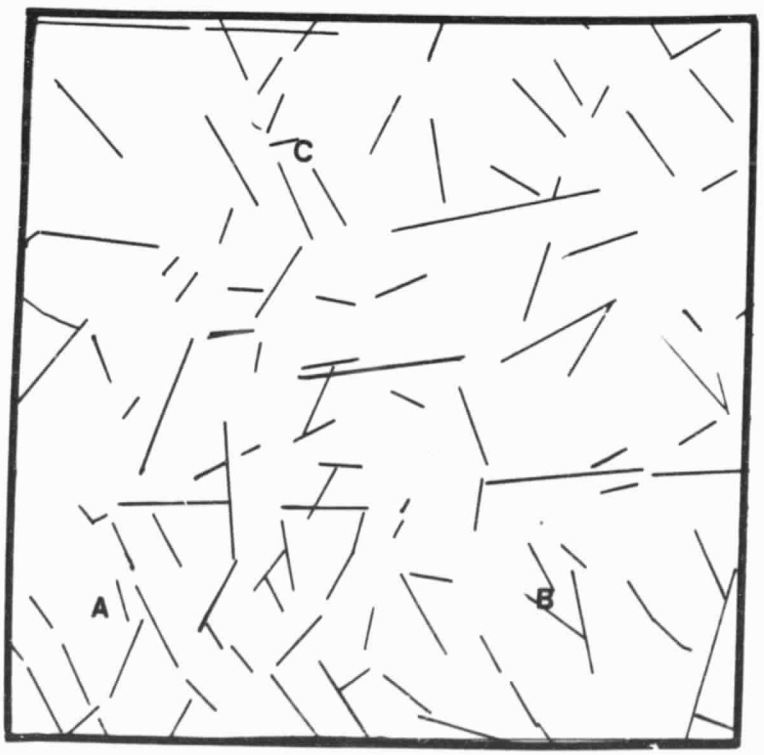

Figure 13B. Lineament map derived from Figure 13A.

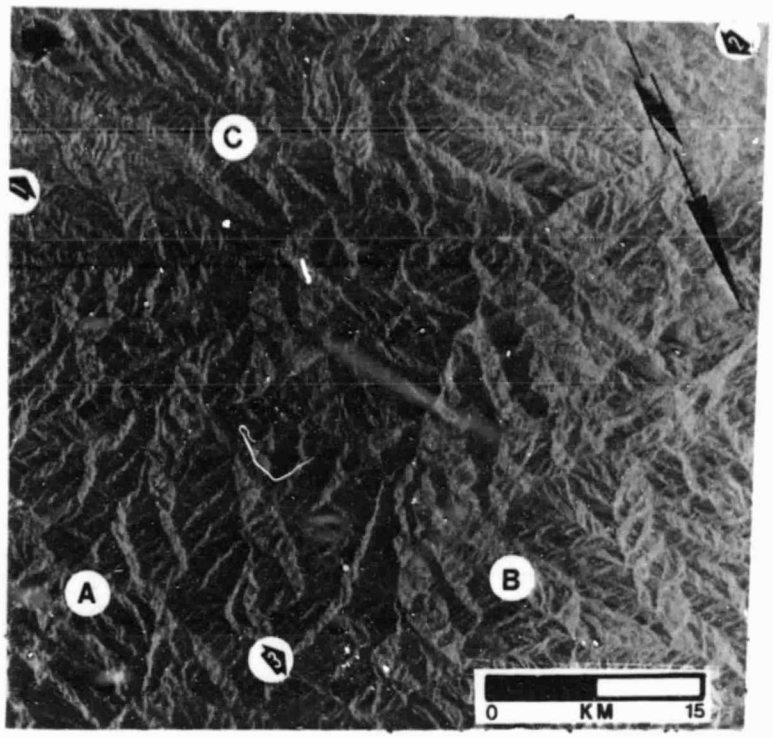

Figure 14A. SIR-A imagery, data take 10-11.

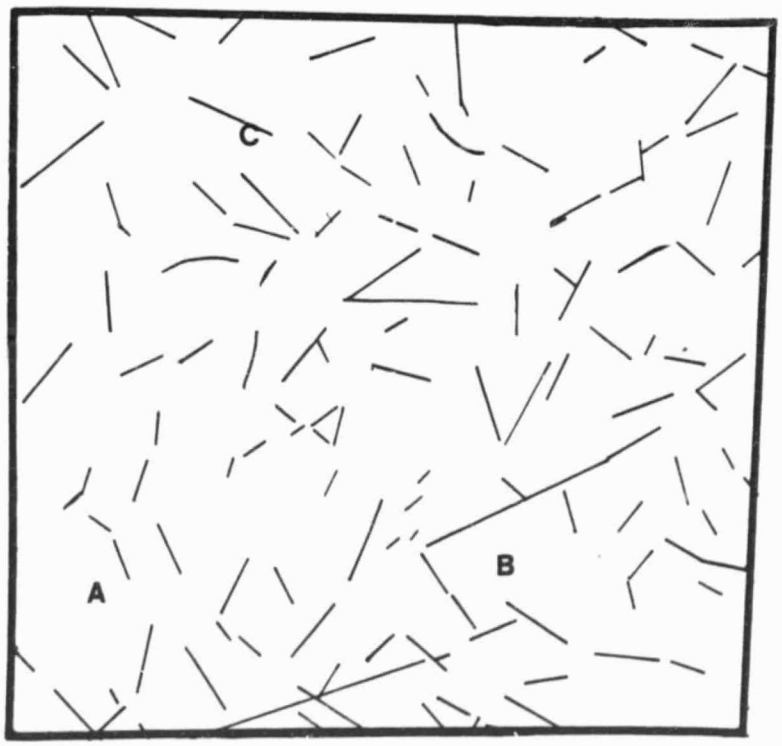

Figure 14B. Lineament map derived from Figure 14A.

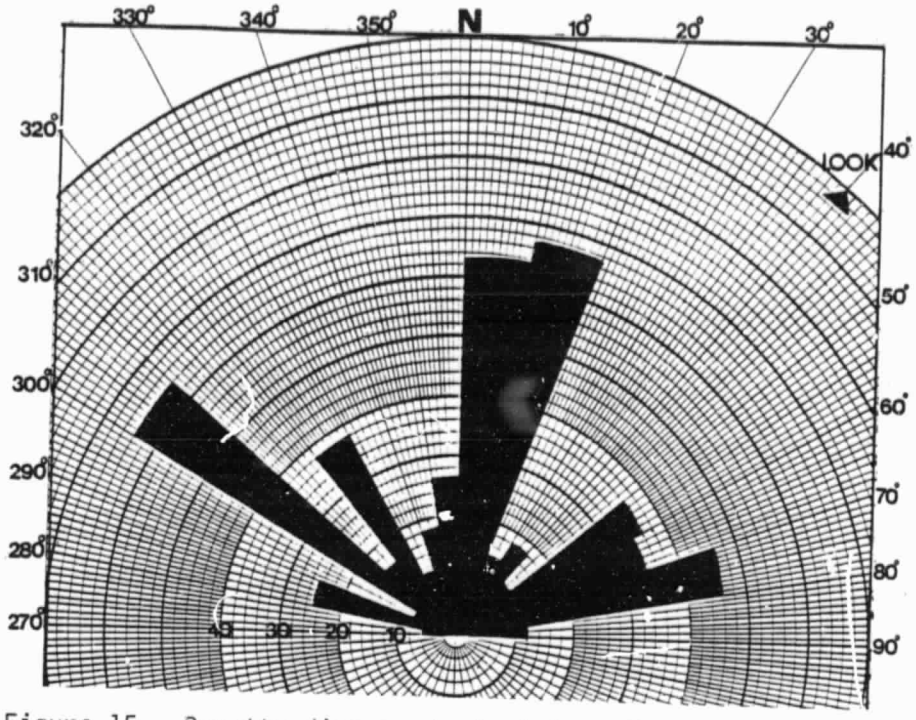

Figure 15. Rosette diagram derived from Figure 13B (data take 24C). Cumulative length in kilometers.

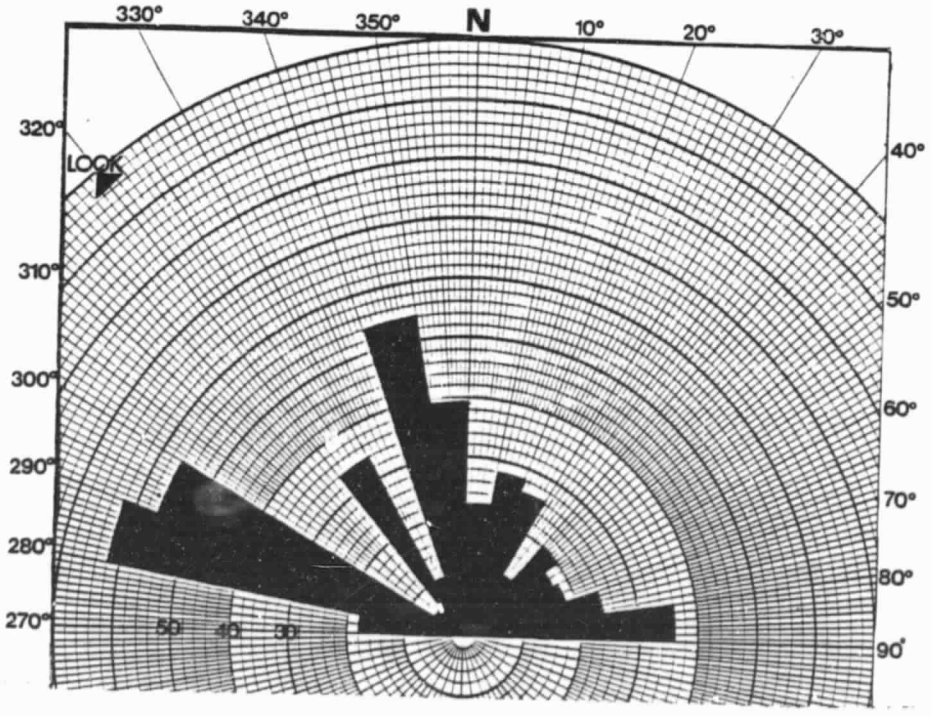

Figure 16. Rosette diagram derived from Figure 14B (data take 10-11). Cumulative length in kilometers.

SECTION 5

NEW GUINEA

Nassau Range, Indonesian New Guinea; Location and General Geology

The Nassau Range which is part of the Sneenuw Mountains (Fig. 1) is located in Irian Jaya which is also called Indonesian New Guinea. The Nassau Range is in the northern half of the study area, whereas the coastal lowlands are located in the southern half. The Nassau Range consists of easterly trending folds of sedimentary strata. The relative relief of the larger folds is approximately 610 m. Extremely low relief (10 m) is typical for the southern coastal plain.

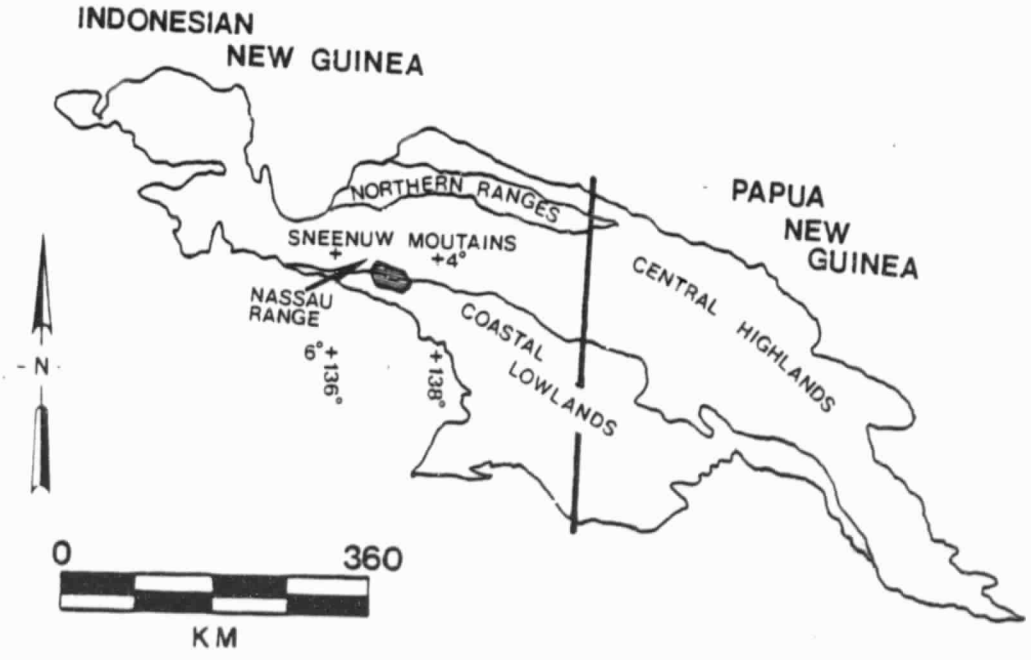

Figure 1. Physiographic provinces of New Guinea. Study area is shaded.

SIR-A Comparisons

Structural axes inferred from three different data sets (SIR-A imagery, Landsat imagery, and aircraft radar imagery) were compared for this study. The structural features interpreted from SIR-A (Figs. 2 and 3) and Landsat (Figs. 4 and 5) are quite similar except in those areas of partial cloud cover recorded on the Landsat image. This result is not unexpected, even though the look-direction of SIR-A (toward northeast) was nearly opposite that of Landsat's solar illumination (toward the southwest). In this

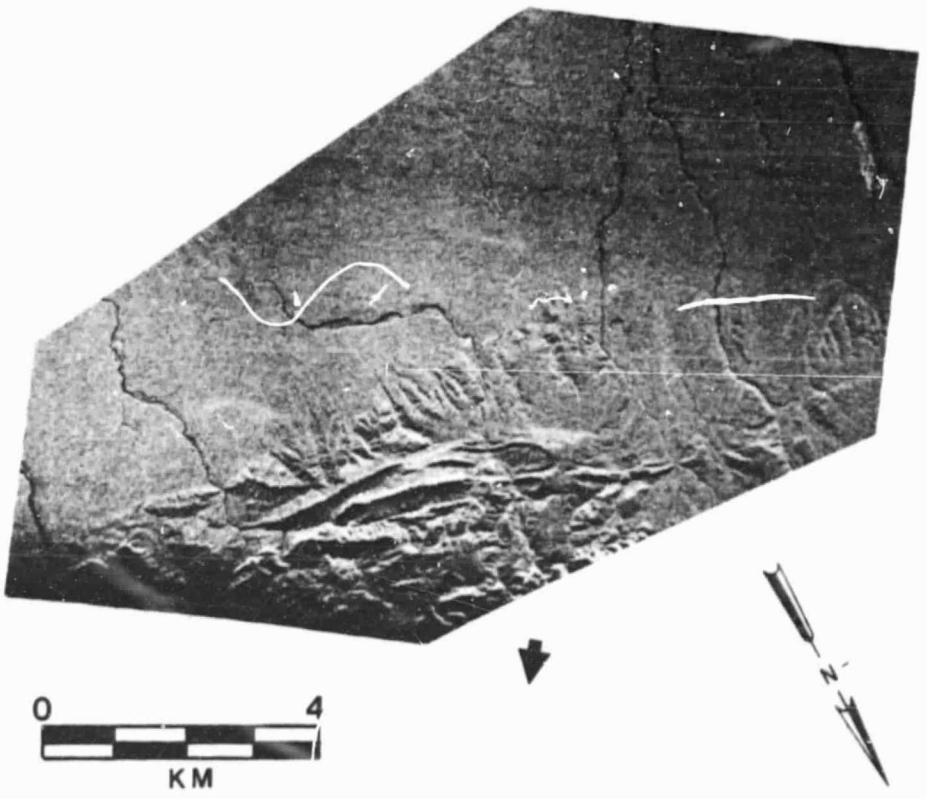

Figure 2. SIR-A image, orbit 29, data take 32-33. Look-direction indicated by arrow.

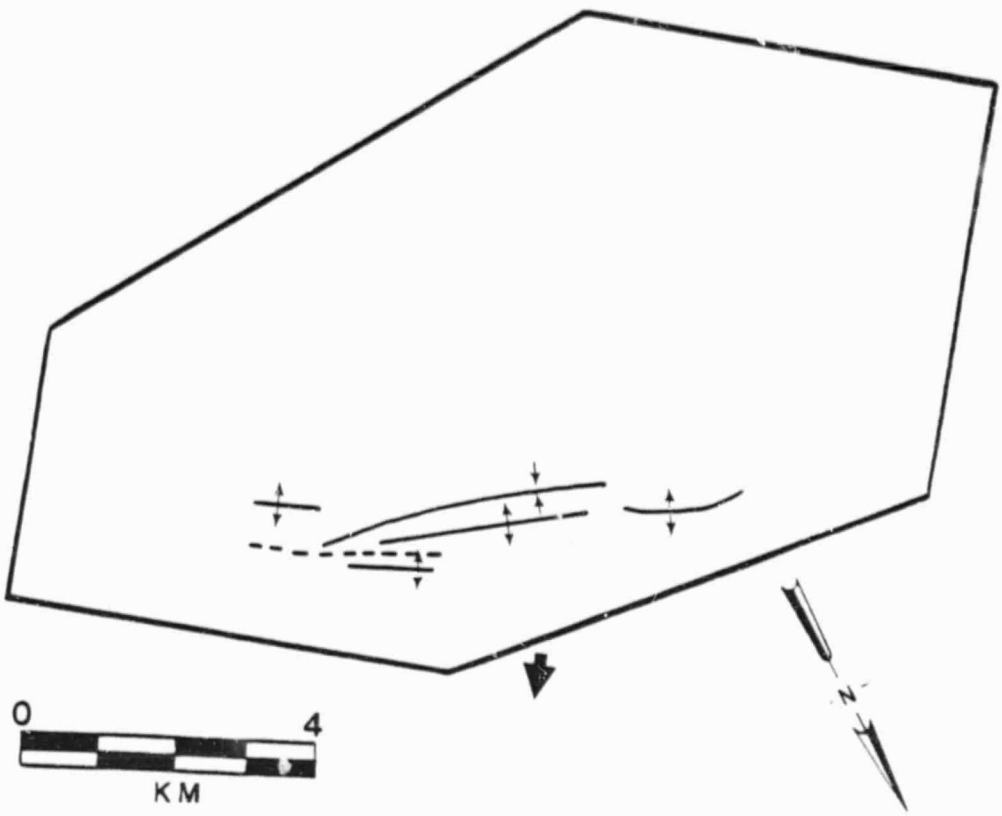

Figure 3. Structural axes map constructed from SIR-A image shown in Figure 2. Look-direction indicated by arrow.

situation, the key to landform enhancement and resultant detection of structural features on SIR-A and Landsat is related to their respective illumination azimuths. The maximum acute angle between look-direction and landform trend, i.e., illumination azimuths, for SIR-A was 80° and for Landsat 70°. These angles approach the optimum viewing angle of near-perpendicular or orthogonal to the structural fabric of the area. Another similarity between the viewing geometry of SIR-A and Landsat is also noteworthy. The SIR-A look-angle of 47°±3° approximates Landsat's look-angle of 40°. To equate the Landsat solar elevation to radar look-angle, the

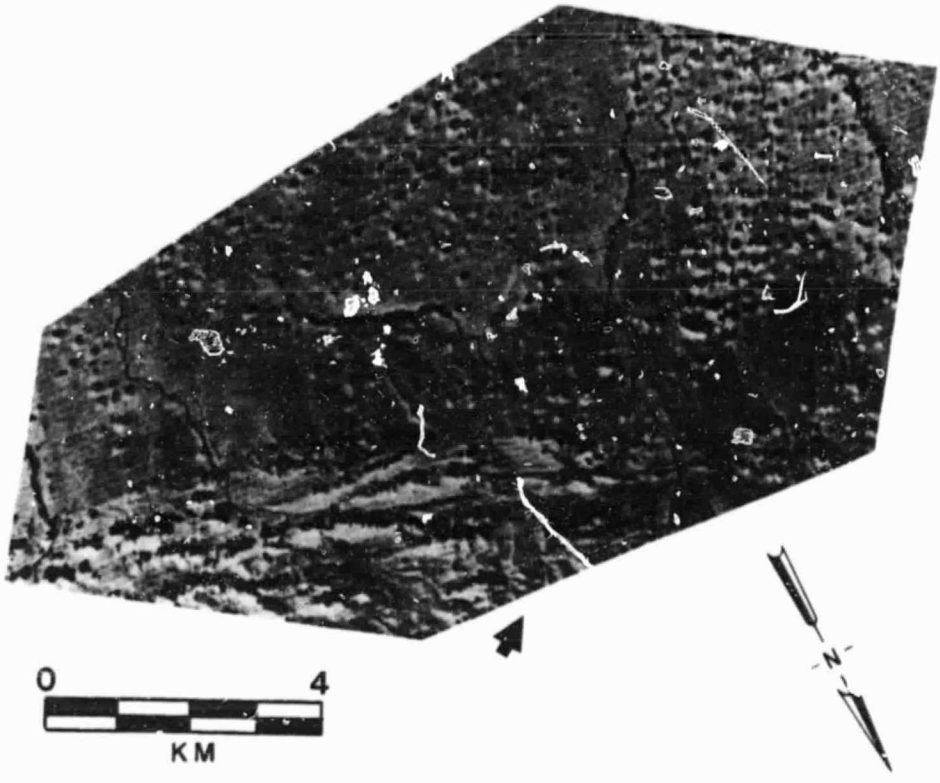

Figure 4. Landsat image of Nassau Mountains area, band 7, April, 1974, solar elevation 50°, solar azimuth 62° (arrow), E-1643-00253-7.

complement of solar elevation is used.

The Ka-band SLAR mosaic (Fig. 6) was constructed from several different aircraft flight lines (swaths) and as a result, variable look-directions and look-angles were used. However, because mid to far range parts of imagery swaths were used in mosaic preparation, look-angles generally exceed 60° throughout most of the imagery illustrated in Figure 6. These relatively larger look-angles appear to be the primary contributing factor for the improvement in geologic interpretability illustrated in Figure 7.

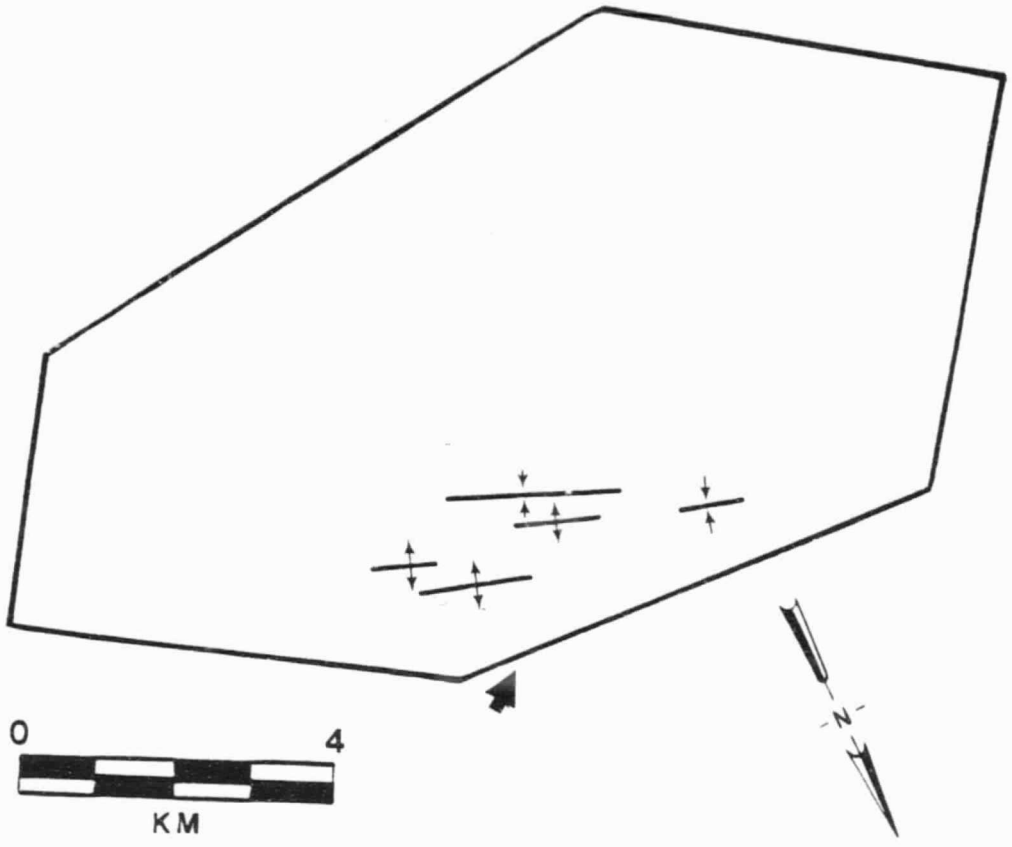

Figure 5. Structural axes map constructed from Landsat image shown in Figure 4. Look-direction indicated by arrow.

Because of the gross size and extent of the features imaged, the relatively better resolution of the aircraft radar is not believed to have a significant impact on improved detectability.

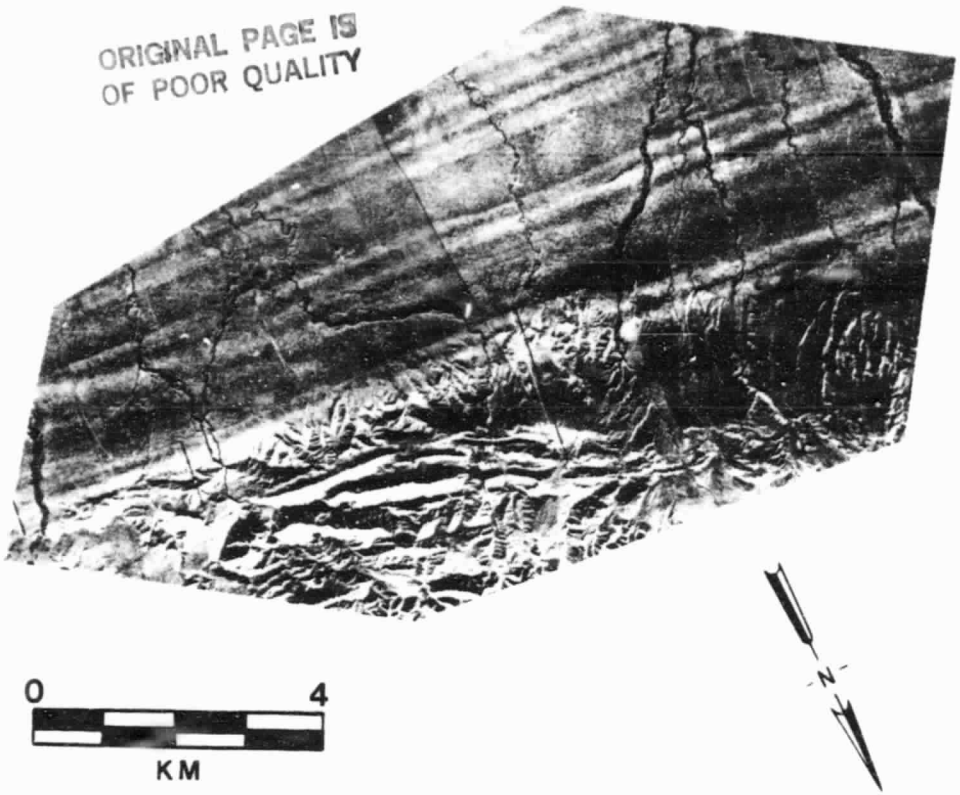

Figure 6. SLAR (Westinghouse AN/APQ-97) mosaic. Look-directions are variable.

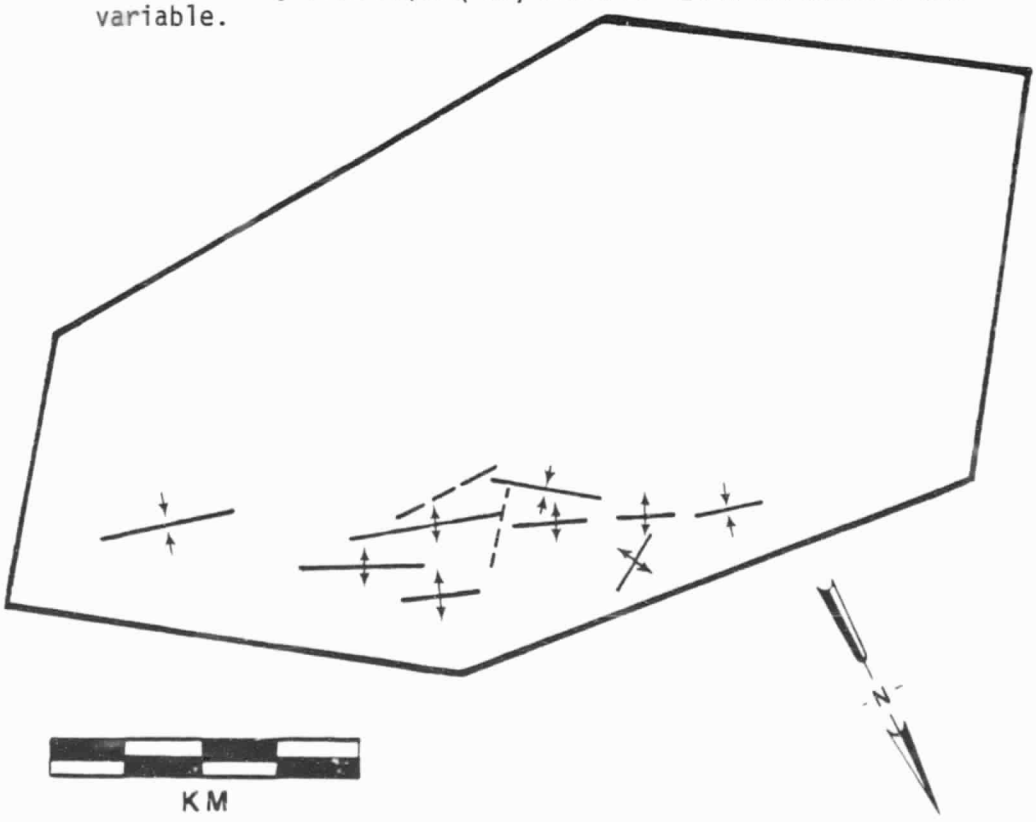

Figure 7. Structural axes map constructed from SLAR image (Fig. 6).

Momats River Area, Indonesian New Guinea, Location and General Geology

The Momats River area (Fig. 8) is located approximately 75 km southeast of the Nassau Range site. Within this coastal lowlands region, the area is extensively covered with a forest vegetation canopy that changes to marsh and swamp plant communities in proximity to the coastline. The average relative relief is less than 10 m.

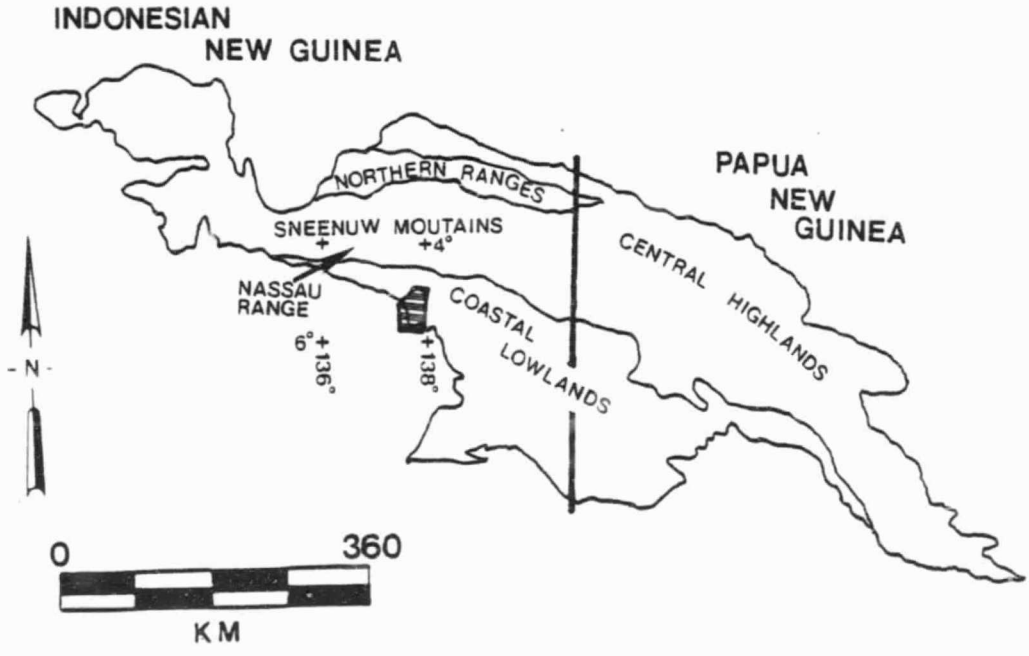

Figure 8. Physiographic provinces of New Guinea. Study area is shaded.

SIR-A Comparisons

Figure 9 provides a Ka-band, aircraft radar mosaic of an area also imaged by SIR-A (Fig. 10). A significant difference in drainage pattern

Figure 9. SLAR (Westinghouse AN/APQ-97) mosaic. Look-direction is variable.

detectability can be observed by comparing SLAR-derived drainage patterns (Fig. 11) with those inferred from SIR-A analysis (Fig. 12). Much of the non-detectability of stream patterns on the SIR-A imagery can be related to the differences in resolution between SIR-A (40 meters) and the aircraft imagery (approximately 15 m). Especially in relatively flat regions (area H, Figs. 9 and 10) where stream or river valley walls have

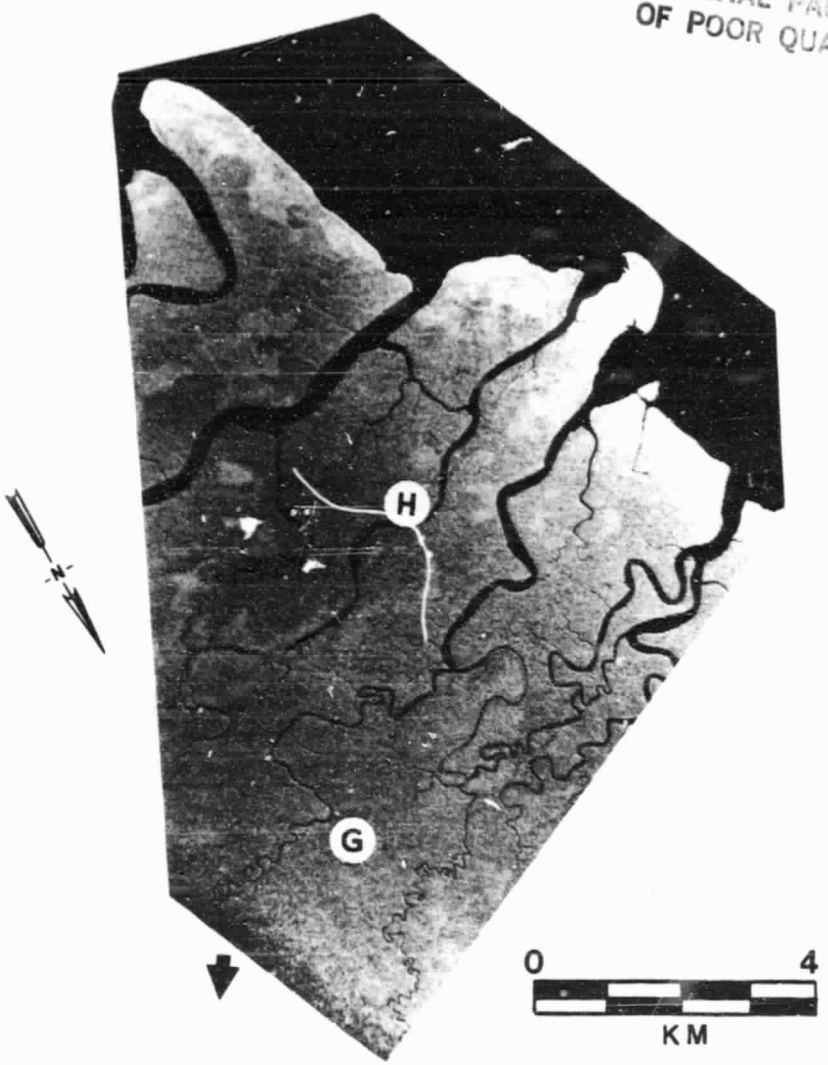

Figure 10. SIR-A image, orbit 29, data take 32-33. Look-direction indicated by arrow.

insufficient slope or relief to be influenced by radar foreshortening or shadow, tonal contrast between open water in stream channels (black) and the surrounding vegetation canopy (gray) appears to be the primary criterion for drainage pattern recognition. On the SIR-A imagery, stream headwaters appear to blend in with the surrounding vegetation and

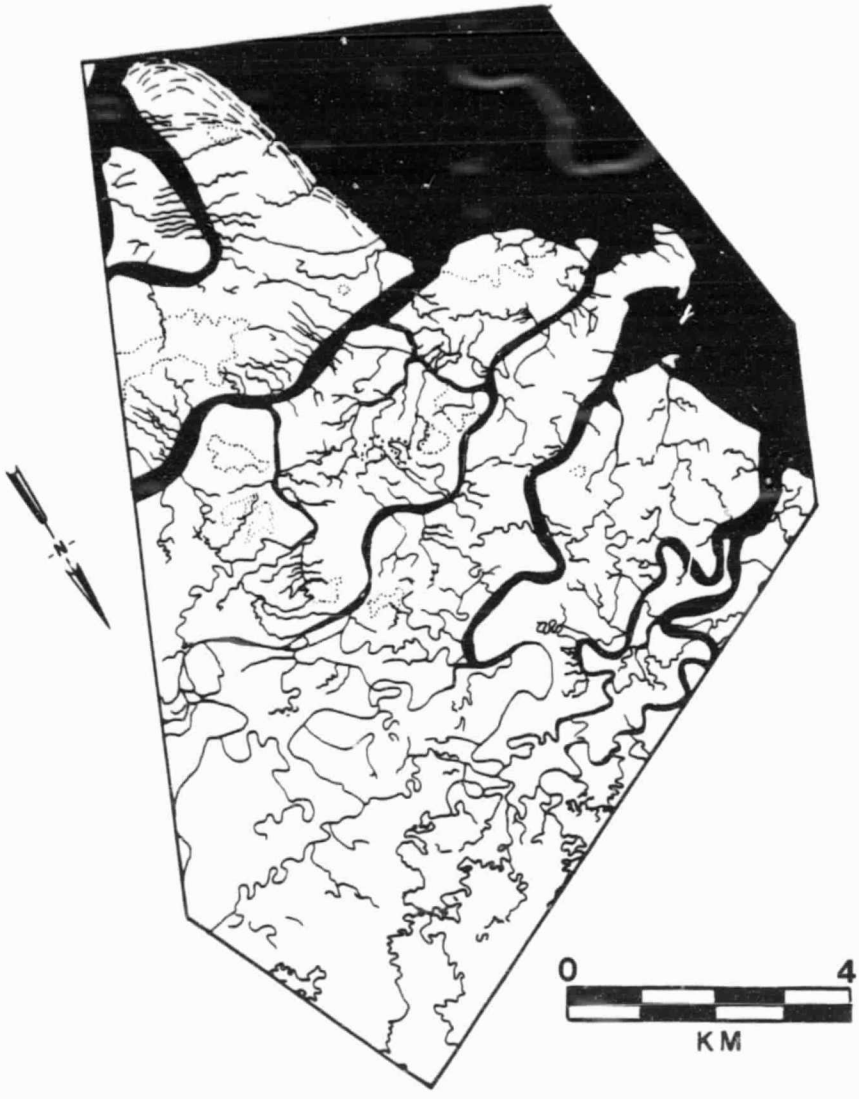

Figure 11. Drainage map constructed from SLAR mosaic shown in Figure 9.

disappear. However, on the SLAR mosaic, the black tonal patterns from open water in the relatively narrow stream channels are still detectable well beyond those points where they disappear on the SIR-A image. Consequently, in this terrain environment, an improvement in resolution has resulted in a better drainage mapping product.

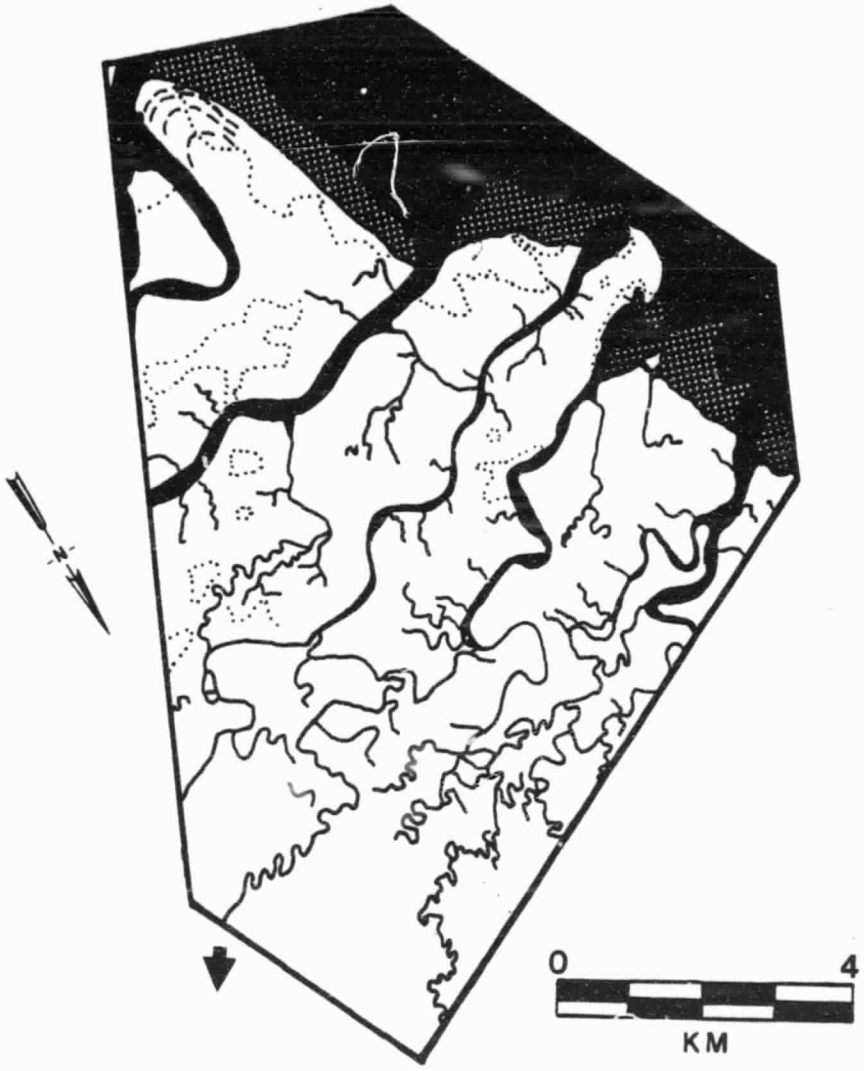

Figure 12. Drainage map constructed from the SIR-A image shown in Figure 10. Look-direction indicated by arrow.

The identification of plant communities using radar imagery often requires identification keys comparable to those used for photo interpretation of the same features, namely tone and texture. Relatively short wavelength radars such as the Ka-band system (0.86 cm) which obtained the

imagery illustrated in Figure 9, are generally more sensitive to the initial surface roughness of a vegetation canopy. In contrast, longer wavelength radars, such as SIR-A's 23 cm system are more influenced by a combination of initial surface and the underlying vegetation volume. Tonal and textural contrasts which can be correlated with boundaries between different plant communities are conspicuous on the shorter wavelength aircraft imagery, and are indicated by dot patterns on Figure 11. Variation in vegetation texture is completely absent on the SIR-A imagery of the same area. However, tonal contrasts on the SIR-A imagery, which correlate in part with plant community boundaries have been indicated by dot patterns on Figure 12.

Mudflats are believed to be the cause of a mottled gray tone observable on the SIR-A imagery. Although these areas could not be reproduced in sufficient detail for this report, the stippled pattern located in offshore areas of Figure 12 indicates the extent of these features as mapped from original imagery. Similar features were not observable on the aircraft imagery. Non-detectability could be related to differing tidal conditions (low tide for SIR-A and high tide during aircraft image acquisition) or simply one of film processing where tonal contrasts are lost during each film generation.

SECTION 6 SUMMARY

Significance of Look-Angle

Landforms, the natural physical features of the Earth's surface, when developed under similar conditions of weathering and erosion, commonly exhibit a predictable range of visual geologic conditions. The sensitivity of radar backscatter to variations in slope and relief can be used, in principle, to map landform features which in turn provide indications of subsurface geology. There is every reason to believe that geologists will use spacecraft radar predominantly for structural/tectonic mapping by empirical correlation with landform geometries. However, optimum retrieval of geologic information to accomplish this task is dependent on tailoring the radar system's look-angle to the local terrain configuration.

Radar imagery comparisons in this study demonstrate the interdependence of radar system geometry and terrain configuration for optimum retrieval of geologic information. We can summarize our knowledge of the importance of look-angle effects on geologic interpretation as follows:

Radar imagery acquired at small look-angles (<30°) can sometimes provide highlighting of subtle slope/relief features; however, these same relatively small look-angles can result in excessive foreshortening and layover in high slope/relief areas. The presentation of mountainous terrain in this angular range severly distorts the geometric fidelity, thereby making such radar imagery only marginally useful for most geologic investigations. Small look-angles are therefore potentially very useful for imaging terrain with low slope/relief characteristics.

Intermediate look-angles suffer from geometric distortions such as relief displacement as well as diminished sensitivity of the electromagnetic characteristics of the terrain. In

the 30°-70° look-angle range, a typical backscatter trend shows a marked reduction in sensitivity to the terrain configuration. Consequently, small angular slope variations associated with subtle landform expression commonly result in imagery having little tonal contrast. Nonetheless, this range of angles is best suited for lithologic analysis where diminished sensitivity to topography is desirable, and for imaging very rough or mountainous terrain where the relief displacement is tolerable and the slope and relief are sufficiently large to create acceptable tonal contrasts in the imagery.

Radar imagery obtained using large look-angles (>70°) provides an image format with greatly reduced foreshortening and layover; however, in high slope/relief areas excessive shadowing may result. Although shadowing dominates the imagery resulting in a loss of information, this angular region of a typical backscatter curve again enjoys a significant change in slope, and provides highlighting of subtle landform features. Therefore, if a space radar can provide sufficient overlap of orbit paths to fill in the shadow areas, a large look-angle configuration seems highly desirable because of the improved fidelity of image format it provides for a wide variety of terrain types.

Look-Angle vrs. Resolution

Published reports commonly support the contention that because of Seasat's improved resolution (25 m) over that of Landsat (79 m), Seasat imagery has generally proved to be superior to Landsat for detecting small-scale terrain features and for mapping high order stream patterns in areas of subdued relief. Evidence provided in this report would suggest that the improvement in aircraft SLAR resolution over that of SIR-A does indeed appear to be a contributing factor for the detectability of higher order stream patterns in relatively flat regions. Especially in the coastal environments of New Guinea, where stream channels have insufficient slope or relief to be influenced by radar foreshortening or shadow, tonal contrasts between open water (black) in the stream channels and the surround-

ing vegetation (gray), appears to be the primary criterion for drainage pattern recognition. However, additional examples illustrated throughout this report provide evidence that in those terrain environments where slope/relief characteristics influence radar return, improvements in landform detection on Landsat imagery over that of SIR-A are not related to resolution. When a properly selected (low sun angle) Landsat image is compared with a SIR-A image, the Landsat scene having the poorest resolution commonly provides for the best terrain enhancement and consequent improved landform definition. Although the fundamental differences in the manner in which solar and radar reradiation interact with the terrain or terrain cover may influence the detectability of landform features, the ability to acquire multiple look-angle/look-direction radar images of a given area appears to be more valuable for landform mapping than further improvements in spatial resolution.

SECTION 7 CONCLUSIONS

The dominant merits of radar remote sensing have long been held to be an active mode of operation, independence from weather and solar illumination, and enhancement of topographic relief (landforms) through highlighting and/or shadowing. Geologists have exploited this capability of imaging radars to detect subtle variations in surface topography which, can sometimes be related to the underlying structural configuration. In this study, comparisons of Landsat MSS imagery, and aircraft and space radar imagery (Seasat and SIR-A) have provided an insight into the importance of multiple look-angle imagery for geologic reconnaissance mapping. Radar imagery comparisons from different geologic environments in the United States, Panama, Colombia, and New Guinea demonstrate the interdependence of radar system geometry and terrain configuration for optimum retrieval of geologic information.

Most recent research in radar geology involves developing geologic models for a multiple data source approach (data merging) to exploit the potential information content of radar backscatter for lithologic or surface materials discrimination. Although this application may have considerable potential in certain geologic environments, there is every reason to believe that geologists will use space radar predominantly for structural and lithologic mapping by empirical correlation with landform geometries of both the imaging system and the terrain. The optimum look-angles for many geologic applications, especially structural/tectonic mapping, are those which enhance the discrimination of surficially ex-

pressed features while minimizing the data loss due to shadowing and excessive geometric distortion. Consequently, the best combination for geologic reconnaissance mapping will vary significantly among different terrain types.

Geologists usually desire relatively good resolution (about 30 m) in orbital imaging systems to provide an improvement in landform discrimination. However, examples illustrated throughout this report would suggest that in the case of space radars (SIR-A in particular), the ability to acquire multiple look-angle/look-direction radar images of a given area is more valuable for landform mapping than further improvements in resolution.

SIR-A will be the first orbital imaging radar system capable of providing multiple images of the same terrain obtained at significantly different look-angles. In addition, SIR-B will also allow variable look-angle coverage of a wide spectrum of landform features in different geologic environments. Used in conjunction with other image types, comparative studies of slope/relief effects on feature perception in multiple SIR-B images will allow a rare opportunity to determine optimum radar look-angles for world-wide geologic applications.